

CHANGES IN EL NIÑO – SOUTHERN OSCILLATION (ENSO) CONDITIONS DURING THE GREENLAND STADIAL 1 (GS-1) CHRONOZONE REVEALED BY NEW ZEALAND TREE-RINGS

Jonathan G. Palmer^{1*}, Chris S.M. Turney¹, Edward R. Cook², Pavla Fenwick³,
Zoë Thomas¹, Gerhard Helle⁴, Richard Jones⁵, Amy Clement⁶, Alan Hogg⁷,
John Southon⁸, Christopher Bronk Ramsey⁹, Richard Staff⁹, Raimund Muscheler¹⁰,
Thierry Corrège¹¹ and Quan Hua¹²

1. School of Biological, Earth and Environmental Sciences, University of New South
Wales, Sydney, New South Wales, Australia.
2. Lamont-Doherty Earth Observatory of Columbia University, Palisades, NY 10964, USA.
3. Gondwana Tree-ring Laboratory, P. O. Box 14, Little River, Canterbury, 7546, New
Zealand.
4. GFZ German Research Centre for GeoSciences, Section 5.2, Telegrafenberg, 14473
Potsdam, Germany.
5. Department of Geography, Exeter University, Devon, EX4 4RJ, UK.
6. Rosenstiel School of Marine and Atmospheric Science, University of Miami, 4600
Rickenbacker Causeway, Miami, FL 33149, USA.
7. Waikato Radiocarbon Laboratory, University of Waikato, Private Bag 3105, Hamilton,
New Zealand.
8. Department of Earth System Science, University of California, Irvine, CA 92697-3100,
USA.
9. Research Laboratory for Archaeology and the History of Art, University of Oxford,
Dyson Perrins Building, South Parks Road, Oxford OX1 3QY, UK
10. Department of Geology—Quaternary Sciences, Lund University, 22362 Lund, Sweden.
11. UMR CNRS 5805 EPOC – OASU, Univ. Bordeaux, 33615 PESSAC CEDEX, France.
12. Australian Nuclear Science and Technology Organisation (ANSTO), Locked Bag 2001,
Kirrawee DC, NSW 2232, Australia.

*Correspondence: J. Palmer. Email: j.palmer@unsw.edu.au

Abstract:

The warming trend at the end of the last glacial was disrupted by rapid cooling clearly identified in Greenland (Greenland Stadial 1 or GS-1) and Europe (Younger Dryas Stadial or YD). This reversal to glacial-like conditions is one of the best known examples of abrupt change but the exact timing and global spatial extent remains uncertain. Whilst the wider Atlantic region has a network of high-resolution proxy records spanning GS-1, the Pacific Ocean suffers from a scarcity of sub-decadally resolved sequences. Here we report the results from an investigation into a tree-ring chronology from northern New Zealand aimed at addressing the paucity of data. The conifer tree species kauri (*Agathis australis*) is known from contemporary studies to be sensitive to regional climate changes. An analysis of a 'historic' 452-year kauri chronology confirms a tropical-Pacific teleconnection via the El Niño – Southern Oscillation (ENSO). We then focus our study to a 1010-year subfossil kauri chronology that has been precisely dated by comprehensive radiocarbon dating and contains a striking ring-width downturn between ~12,500 to 12,380 cal BP within GS-1. Wavelet analysis shows a marked increase in ENSO-like periodicities occurring after the downturn event. Comparison to low- and mid-latitude Pacific records suggests a coherency in the changes to ENSO and Southern Hemisphere westerly airflow during this period. The drivers for this climate event remain unclear but may be related to solar changes that subsequently led to establishment and/or increased expression of ENSO across the mid-latitudes of the Pacific, seemingly independent of the Atlantic and polar regions.

Highlights:

- Century-duration climate shift identified ~12,500 to 12,380 cal BP within the Greenland Stadial-1 chronozone
- El Niño - Southern Oscillation expressed Pacific Ocean-wide after ~12,380 cal BP
- Pacific-wide change do not appear to be driven by the North Atlantic

Keywords:

Dendrochronology; New Zealand kauri (*Agathis australis*); abrupt climate change; Greenland Stadial 1 (GS-1); Younger Dryas (YD); Antarctic Cold Reversal (ACR); Last Termination.

1. Introduction

The interruption of long-term warming towards the end of the last glacial termination (18-10 ka BP) and a return to cold, arid conditions in Europe has been commonly described as the Younger Dryas (YD) Stadial (Walker et al., 1999). More widely in the North Atlantic the broadly synchronous change is referred to as the Greenland Stadial-1 (GS-1; 12.9 to 11.65 ka BP) (Björck et al., 1996; Blockley et al., 2012; Brauer et al., 1999; Lynch-Stieglitz et al., 2014; Mayle et al., 1999; Muschitiello et al., 2015; Rasmussen et al., 2014; Walker et al., 2003), traditionally considered to have been driven by a sustained reduction of North Atlantic Meridional Overturning Circulation (AMOC) (Carlson and Clark, 2012; Carlson et al., 2007; Muschitiello et al., 2015; Renssen et al., 2015; Tarasov and Peltier, 2005). Although the GS-1 may have extended hemispheric-wide (Bronk Ramsey et al., 2012; Cooper et al., 2015; MacDonald et al., 2008; Wang et al., 2001; Williams et al., 2002; Yoshida and Takeuti, 2009), the spatial and temporal expression of climate during this period remains complex with an anti-phase trend in temperature between the high-latitudes postulated to be evidence for a bipolar ocean seesaw (Broecker, 1997; EPICA Community Members, 2006; Stocker and Johnsen, 2003; WAIS Divide Project Members, 2015). Importantly, whilst marked climate variability is recorded across the North Atlantic during GS-1 (Bartolomé et al., 2015; Lane et al., 2013; Lowe, 2001; Rach et al., 2014) there is evidence for low latitudes leading the change (Partin et al., 2015; Steffensen et al., 2008) suggesting mechanism(s) other than oceanic forcing may have played the driving role. To help better understand the drivers and transmission of abrupt and extreme change across GS-1 (and the last glacial period more generally), high-resolution records that capture modes of variability are required to provide a more complete global picture.

Atmosphere-ocean interactions in the central tropical Pacific are considered to have a major influence on contemporary global climate change (Kosaka and Xie, 2013; Tierney et al., 2015; Turney et al., 2015). Arguably the best known is the El Niño-Southern Oscillation (ENSO), characterised by cool (La Niña) and warm (El Niño) phases that operate on inter-annual (2.5-7 years) (Collins et al., 2010; Tudhope et al., 2001) timescales with severe and wide-reaching impacts on ecosystems and societies (Buckley et al., 2010; Iizumi et al., 2014; McPhaden et al., 2006; Turney and Hobbs, 2006). Although equatorial marine sedimentary records (Koutavas and Joanides, 2012; Leduc et al., 2009; Sadekov et al., 2013) and modeling studies (Liu et al., 2014) appear to show relatively high ENSO variance and stable teleconnections across the last glacial period, there is a relative dearth of annually-

resolved and well-dated records in the low to mid latitudes of the Pacific Ocean to test these hypotheses. In New Zealand, sedimentary records appear to capture the mid to high Southern Hemisphere latitude warming trend coincident with GS-1 but are of insufficient resolution to detect ENSO variance (Barrell et al., 2013; Doughty et al., 2013; Jara et al., 2015; Lowe et al., 2013; McGlone et al., 2010; Pedro et al., 2016; Turney et al., 2006; Turney et al., 2003; Vandergoes et al., 2008). Only one fragmented laminated sequence (Onepoto Maar, Auckland Volcanic Field) appears to preserve a record of modern-like ENSO variability across the last glacial (Pepper et al., 2004) but the sections are of centennial-scale duration and do not span the GS-1 chronozone, precluding a global perspective (Corrège et al., 2004; Reeves et al., 2013; Rodbell et al., 1999). Tree-ring records are an ideal alternative. Whilst some tropical tree species have demonstrated annual resolution and sensitivity to climate (e.g. Baker et al., 2008; Brien et al., 2016; Schollaen et al., 2013), no multi-millennia length chronologies have been reported for this period. Fortunately, however, some sub-tropical locations appear to exhibit atmospheric teleconnections to the tropics.

New Zealand kauri trees (*Agathis australis*) produce annual rings sensitive to climate (Boswijk et al., 2006; Buckley et al., 2000; Fowler et al., 2000; Palmer and Ogden, 1983), with most of their growth in the austral spring and early summer and a demonstrated ability to reconstruct changes in ENSO (Fowler et al., 2000; Fowler et al., 2012). Over the past three decades, a collection of subfossil ‘ancient’ (late Pleistocene) kauri log samples (<60 ka BP) has been assembled (Hogg et al., 2006; Ogden et al., 1993; Palmer et al., 2006; Palmer et al., 2015a; Turney et al., 2010), offering considerable insights into the climate system (Turney et al., 2016b). We know of nowhere else in the world with such a rich resource of long-lived subfossil trees that are older than the Holocene. Some of the buried trees are of enormous proportions, with diameters extending to 4 metres and individual tree-ring counts giving ages of more than 2000 years (Palmer et al., 2006). As a result of the quantity of preserved logs and timber quality, the buried wood is being ‘harvested’ for commercial purposes, providing the unique opportunity for sample collections and the development of multi-millennial chronologies.

Recently, a decadal-resolved radiocarbon (^{14}C) sequence obtained from a 1771-year long ancient New Zealand kauri (*A. australis*) tree-ring series was reported (Hogg et al., 2016), providing the first absolutely-dated radiocarbon calibration curve across GS-1. The atmospheric record of ^{14}C preserved in the kauri covers the time range ~13,134-11,363 cal

BP, allowing high-precision alignment of floating Northern Hemisphere tree-ring records (with a maximum 1-sigma uncertainty of ± 8 calendar years) (Kaiser et al., 2012; Kromer et al., 2004) back to 14,174 \pm 3 cal BP. The data provided by Hogg et al. (2016) showed that the interhemispheric atmospheric ^{14}C offset was close to zero prior to GS-1 before reaching ‘near-modern’ values at \sim 12,660 cal BP. The results are consistent with a synchronous recovery of overturning in both hemispheres and increased Southern Ocean ventilation. Crucially, comparison of radiocarbon in the tropical annually-laminated Cariaco Basin (Hughen et al., 2004; Southon et al., 2012) has allowed the identification of two relatively short periods of AMOC collapse, at \sim 12,920-12,640 cal BP and 12,050-11,900 cal BP, suggesting opposing hemispheric temperature trends were driven by atmospheric teleconnections (Hogg et al., 2016).

Here we explore the ocean-atmospheric drivers of ‘modern’ kauri using the NOAA-CIRES Twentieth Century Reanalysis Project (20CR version 2c) (Compo et al., 2011) to help interpret the palaeoclimate information gleaned from the well-replicated portion of the kauri tree-ring chronology (i.e. 1010-years out of the original 1771-year sequence) collected from northern New Zealand. Our analysis provides new insights into Pacific-wide changes during the end of the last glacial period.

2. Methods

2.1 *Modern kauri*

Before discussing the palaeoclimate signals in the subfossil kauri sequence we first review the “modern” kauri climatic response. A modern master kauri tree-ring chronology was developed using a sample pool of 428 tree-ring series from 15 sites located across the upper North Island of New Zealand (Boswijk et al., 2014; Figure 1 and Table 1) available from the data archive at the International Tree-Ring Data Bank (the ITRDB; www.ncdc.noaa.gov). The sample pool of sites effectively spans the natural range of the species and the individual series were selected on the basis of their level of correlation to one another using the program COFECHA (Grissino-Mayer, 2001). This approach was considered preferable to the alternative of deriving the modern master by combining individual site chronologies. Large inter-site differences in sample depth would have been of concern (Fowler et al., 2004) but this adopted approach permitted the incorporation of additional material (such as from Mount Moehau) that would have been otherwise omitted as a site. To reduce the possible effects of tree-ring index inflation bias (Cook and Peters,

1997) the measurement series were first power-transformed and then a 200-year spline was subtracted to produce residual indices. The series were then run through the “signal free” method of tree-ring standardization (Figure 2a; Melvin and Briffa, 2008) to overcome possible problems of trend distortion seen especially at either end of the chronology. The final modern chronology spans the period CE 1269 to 2002 but previous studies have shown that the early portion of the kauri chronology should be considered unreliable unless there are ring-width series from at least 20 trees included (Fowler et al., 2008). Their result was based on calculations of the expressed population signal, or EPS, being greater than 0.85 (Wigley et al., 1984). Using the tree-ring program ARSTAN (Cook, 1985; Cook and Kairiukstis, 1990) we selected to analyse the strength of the common signal from both within and between different trees over a common time interval. The primary reason for doing this was to corroborate earlier findings (Fowler et al., 2008) and determine the number of samples needed to produce a “robust” chronology. The common window of time chosen for the modern kauri chronology was from CE 1676 to 1975 (i.e. a 300 year span) with the EPS results indicating that 21 trees are needed; therefore only the portion starting from CE 1550 was used (Figure 2a, b). We then explored the spectral pattern of the chronology by using the R-package “biwavelet” (Gouhier et al., 2016) with the results shown in Figure 2c.

The strength of the climate signal in the modern kauri chronology was evaluated by comparisons to the Southern Oscillation Index (Ropelewski and Jones, 1987), TriPole Index of the Interdecadal Pacific Oscillation (TPI; (Henley et al., 2015), Niño 3.4 sea-surface temperatures from the Hadley Centre Global Sea Ice and Sea Surface Temperature (HadISST; (Rayner et al., 2003), and the Southern Annular Mode (Marshall, 2003). The program PCReg (www.ldeo.columbia.edu/tree-ring-laboratory) was used to carry out a linear regression model of the tree-ring chronology to the selected climate window. Each climate record period was split in half so that strictly independent calibration and validation testing could be undertaken (Table 2; (Cook and Kairiukstis, 1990) and was based on the austral four-season climate year starting in winter (June) and ending in autumn (May). Two rigorous tests of the regression models performance, the reduction of error (RE) and the coefficient of efficiency (CE) were calculated (Table 2; (Cook and Kairiukstis, 1990).

2.3 Towai Farm site and subfossil chronology development

1 A cohort of 39 sub-fossil kauri logs were discovered at a farm site near Towai
2 (35°30.393'S, 174°10.376'E; Figure 1) in Northland. Unlike some other known sites with
3 subfossil kauri (Palmer et al., 2006), all the logs unearthed on this farm had been buried
4 during a similar time period. The trees did not all die at the same time and were not
5 entombed as a result of one single catastrophic event (Figure 3). Rather, an irregular series
6 of mortality events occurred where whole trees (including the root plate) fell over probably
7 as a result of intermittent strong winds across the period of kauri occupation at the site
8 (Lorrey and Martin, 2005). Towards one margin of the peat bog on the property, some
9 scattered and relatively small monoao (*Halocarpus kirkii*) logs were also extracted;
10 radiocarbon dating shows that the monoao trees grew alongside the kauri at the same time
11 (ages not reported here). The peat bog area forms flat farm paddocks that are surrounded by
12 rolling hills consisting of palaeodunes. Ditches were cut several decades ago to convert the
13 peat bog area into flat paddocks for cattle grazing, draining the water from the eastern side
14 of the Northland isthmus to the west (Kaipara Harbour) via the 150 km long Wairoa River.
15 No other logs have been found in neighboring properties that generally have all been
16 drained and “improved” for farming much earlier than Towai Farm.

17 Once excavated, the logs were stockpiled and then transported to a storage yard at the
18 mill where a biscuit or cross-section was provided for tree-ring analysis. Since the biscuits
19 were too large to prepare for tree-ring analysis and measurement, radial strips were first cut
20 out and the surface then repeatedly sanded to produce a finely polished surface following
21 widely used methods (Stokes and Smiley, 1968). The tree-rings in each radial strip were
22 studied under a microscope then measured and the crossdating accuracy evaluated using the
23 program COFECHA (Grissino-Mayer, 2001). The ring-width series were then transformed
24 into indices following the same process as described earlier for the modern chronology
25 (Section 2.1). Of the 39 logs sampled, 37 were successfully crossdated and their ring-width
26 measurements used to develop a floating chronology (see Supplementary Data). The
27 number of trees required to produce a floating chronology with reliable replication in terms
28 of having an EPS greater than 0.85 was approached the same way as done for the modern
29 chronology. In this case the average correlation value between the different series (\bar{r} ,
30 Table 1) was stronger than that seen in the modern chronology with the result a sample
31 depth of only 9 trees is required before the 0.85 EPS threshold is exceeded. One possible
32 reason for this difference is because Towai is a single site whilst the modern chronology is a
33 regional amalgamation with differing site characteristics adding “noise” to the mean

1 chronology. The final result was a floating chronology with reliable replication spanning
2 1,010 years. This floating chronology is locked on to the calendar time-scale (12,959 to
3 11,949 cal BP) by an intensive radiocarbon dating programme reported previously (Hogg et
4 al., 2016).

5 *2.3. The Towai sedimentary sequence*

6 Alongside the excavation of the sub-fossil wood, we dug a shallow pit and using
7 monolith tins and a 8 cm diameter 'D'-section corer sampled a 6.23 m sequence of peats,
8 clays and organic-rich lake mud (gyttja) sediments. The sediments were described using a
9 modified Troels-Smith method (Kershaw, 1997). The sub-fossil material was obtained from
10 the uppermost organic unit down to a depth of 100 cm which was capped by a 20 cm thick
11 clay layer. The uppermost part of the sequence (down to 340 cm) was contiguously sampled
12 every centimetre for organic matter content (loss-on-ignition or LOI) by heating at 550°C in
13 a muffle furnace for two hours. To provide a geochronological framework from the
14 sedimentary sequence we radiocarbon dated different components in the sequence. Bulk
15 peat and terrestrial plant macrofossils (wood) were extracted from the peat sequences and
16 given an acid-base-acid (ABA) pretreatment. Most of the samples were combusted and
17 graphitized in the University of Waikato AMS laboratory, with $^{14}\text{C}/^{12}\text{C}$ measurement by the
18 University of California at Irvine (UCI) on a NEC compact (1.5 SDH) AMS system. The
19 pretreated samples were converted to CO_2 by combustion in sealed pre-baked quartz tubes,
20 containing Cu and Ag wire. The CO_2 was then converted to graphite using H_2 and a Fe
21 catalyst, and loaded into aluminum target holders for measurement at UCI. This was
22 supplemented by radiocarbon ages measured at the University of Oxford where combustion
23 was undertaken in an Elemental Analyser at 1000 °C, followed by graphitization (involving
24 H_2 reduction of CO_2 to pure C, graphite, over an Fe catalyst (Vogel et al., 1984) for 6 hr at
25 560 °C (Dee and Ramsey, 2000) and measurement using a HVEE tandem accelerator mass
26 spectrometer (Bronk Ramsey et al., 2004).

27 The radiocarbon ages were used to develop an age model using a P_sequence deposition
28 model in OxCal 4.2 (Bronk Ramsey, 2008; Bronk Ramsey, 2011) and the Southern
29 Hemisphere radiocarbon calibration data (SHCal13; (Hogg et al., 2013). Using Bayes'
30 theorem, the algorithms employed sample possible solutions with a probability that is the
31 product of the prior and likelihood probabilities. Taking into account the deposition model
32 and the actual age measurements, the posterior probability densities quantify the most likely

age distributions; the ‘General’ outlier option was used to detect ages that fall outside the calibration model for each group, and if necessary, down-weight their contribution to the final age estimates. Modelled ages are reported here as thousands of calendar years BP or cal BP (Table 2).

2.4. Tipping Point Analysis

To investigate the climate signal of the tree-ring chronology further, we undertook ‘tipping point’ analysis across the period represented by the data preceding the downturn. If abrupt climate changes are driven by long-term forcing, early warning indicators can be mathematically detected by looking at the pattern of fluctuations in the short-term trends of the data prior to the shift (Dakos et al., 2008; Thomas et al., 2015). The method assumes that the system dynamics, as represented by the kauri ring index, are governed by an effective stochastic dynamics with underlying forcing; precursors are not expected in the case of tipping induced by stochastic fluctuations only. Whilst ecological and/or palaeoclimate records are often too sparse to estimate spectral shifts and consequently not provide sufficient resolution for detecting changes (Carpenter and Brock, 2006), tree-rings provide annually-resolved records which allow detection of these changes. These early warning indicators can be manifested through a phenomenon called ‘critical slowing down’, whereby as the threshold or ‘bifurcation’ is approached the climatic response to perturbations become increasingly slow (Dakos et al., 2012; Dakos et al., 2008; Held and Kleinen, 2004). From a dynamical perspective, the basin of attraction (describing the stability of the climate system) becomes gradually wider and shallower (van Nes and Scheffer, 2007), causing the recovery of the system to equilibrium after perturbations to become increasingly longer, which is detected as an increase in the lag-1 autocorrelation and variance of the time series (Lenton et al., 2012). Alternatively, if the system is characterised by high levels of stochastic noise, the system may flicker between two quasi-stable states (Dakos et al. 2013; Thomas and Jones 2016). Patterns in generic indicators such as autocorrelation and variance are also observed, and while an increase in variance is universally detected (Carpenter and Brock 2006; Dakos et al. 2013), autocorrelation may either increase (Dakos et al. 2012; Lenton et al. 2012) or decrease (Wang et al. 2012). To find these statistical properties in the data, the timeseries must be pre-processed to remove the long-term trends in the data using a Gaussian kernel smoothing filter over a suitable bandwidth (such that the long term trends are removed without overfitting the data) (Dakos

et al., 2008). The resulting residuals are then measured for autocorrelation at lag-1 and variance over a sliding window of 50% of the length of the dataset, using the R software functions *ar.ols()* and *var()*, respectively (R Core Team, 2015). A quantitative measure of the trend is provided by the Kendall tau rank correlation coefficient (Kendall, 1948) which assesses the predominance of concordant pairs, providing an objective evaluation of the statistical evidence for the trend. To determine whether the results are sensitive to these parameter choices, we generated running repeats of the analysis with a range of smoothing bandwidths (5-15% of the time-series length) and sliding window sizes (40-60% of the time-series length). The results are visualized using contour plots of the Kendall tau values of these repeats. To determine the significance, we created a surrogate dataset by randomising the original data over one thousand permutations, following Dakos et al. (2008). This method removes any ordered structure or linear correlation while guaranteeing the same amplitude and time probability distribution as the original time series (Theiler et al., 1992), and provides a robust null model, with corresponding results for other approaches used to generate surrogate data (Dakos et al., 2008). The autocorrelation at lag-1 and variance were computed for each of the surrogate time series, and the probability of making a Type I statistical error (i.e. false-positive) for the original data was computed by comparing to the probability distribution of Kendall tau values to those of the surrogate data. A histogram is used to illustrate these results; if the data that we find falls outside the 95th percentile of the surrogate data, our results are significant at $p \leq 0.05$.

3. Results and Discussion

3.1. Modern kauri response to climate

Numerous papers have documented the developments of the modern kauri chronology network with the latest being the update on efforts to extend the modern record back into the mid-Holocene (Boswijk et al., 2014). A repeated caution has been the need for adequate sample depth before climate interpretations can be considered. Our modern kauri chronology has proved no different with the EPS value indicating similar numbers of tree samples being required as previously reported (Fowler et al. 2008). The results highlight the potential problems associated with relatively short samples from sites with modest common signal strength (as reflected in the \bar{r} value, Table 1).

The comparisons of the modern kauri chronology to ENSO and Southern Hemisphere mid-latitude westerly airflow (as measured by the Southern Annular Mode or SAM)

1 produced similar results to those previously reported (Fowler et al. 2000, 2012; Fowler
2 2008). Previous work has demonstrated a relationship of modern kauri to the Tahiti-Darwin
3 Southern Oscillation Index (SOI) (Fowler et al., 2000) and similarly the partitioning
4 analysis results of the SOI quintiles (Fowler et al., 2008) showed significant correlations to
5 their master kauri chronology. Our results reaffirm the previous findings in terms of the
6 strongest contemporary climate relationship with kauri growth is seen with SOI (Table 2).
7 The recently developed tripole index (TPI) of the Interdecadal Pacific Oscillation (Henley et
8 al., 2015) performed better than the sea surface temperature (SST) record of Niño 3.4 but
9 was still less significant than that found for the SOI (Table 2). Importantly, these
10 correlations are supported by spatial regressions that demonstrate a statistically significant
11 relationship between increased tree growth and equatorial Pacific sea surface temperatures
12 (HadISST) (Rayner et al., 2003) centred on the Niño 3.4 and 3 regions (Figure 1), consistent
13 with our correlations (Table 2).

14 Previous detailed work discussed concerns about the reliability of ENSO event detection
15 using kauri data quintiles and also significant outliers (Fowler et al., 2008). To investigate
16 the synoptic conditions that might explain this relationship we interrogated the 20CR 2c
17 (Figure 4; Compo et al., 2011; Cram et al., 2015). Previous work has demonstrated that
18 warming of the central tropical Pacific (El Niño) is associated with anomalously low
19 pressure to the northeast of New Zealand and relatively higher pressure over Australia,
20 partially as a consequence of the contraction of Hadley Cell circulation (Lu et al., 2008),
21 causing a northward displacement of Southern Hemisphere westerlies (Trenberth and Shea,
22 1987). As a result, a higher incidence of cold fronts delivers southerly cool dry airmasses
23 over Northland (Gordon, 1985; Ummenhofer and England, 2007). Here we find that growth
24 is enhanced under more southerly airflow, primarily associated with relatively lower
25 atmospheric pressure northeast of New Zealand, though reduced cloud cover (increasing
26 solar radiation) may also play a role (Fowler et al., 2000). An optimal response to regional
27 circulation changes is observed with a lag of two months between synoptic conditions (July-
28 December) and kauri growth (September-February), associated with more southerly airflow
29 extending over Tasmania (Figure 4).

30 With the above results we consider the use of power-transformed residuals for the kauri
31 tree-ring standardisation helps address some earlier concerns (Fowler et al., 2008).
32 Furthermore, as previously noted, the modern multi-site chronology comes from only a
33 small and remote region outside of the core equatorial Pacific zone of ENSO which is

1 known to be spatially variable (Fowler et al., 2008) making New Zealand kauri highly
2 sensitive to tropical–mid-latitude teleconnections. That said, the results presented in Table
3 2 confirm the presence of an ENSO signal in kauri and the jack-knife
4 calibration/verification results demonstrates that this response appears stable over the
5 instrumental record.

6 One aspect not previously looked at with kauri climate responses has been the effect of
7 the IPO on modulating the expression of ENSO. In particular, asymmetric responses in
8 Australian climate variations to ENSO during different phases of the IPO has been
9 demonstrated in relation to extreme events in eastern Australia in observations and models
10 (Cai et al., 2012; Kiem et al., 2003; King et al., 2013; Power et al., 1999) and possibly New
11 Zealand (Jiang et al., 2013; Salinger et al., 2001). To explore this, we plotted the linear
12 regression between the SOI and the modern kauri master from 1877-2002, stratified by the
13 polarity of the IPO phase (Figure 5; (Power et al., 1999). This figure shows the IPO phases
14 do not unduly influence the SOI response of kauri. Neither the slope nor the regression
15 significance changed significantly between phases so the kauri response (albeit modest) can
16 be considered consistent and stable during both positive and negative IPO phases.

17 The spectral pattern of the modern chronology (Figure 2c) is very similar to earlier
18 studies that have reported comparable 2.5-7 years ENSO periodicity (Fowler et al., 2012)
19 (Kestin et al., 1998; Tudhope et al., 2001; Xie et al., 2015), one that straddles more than the
20 Niño 3.4 region (Kao and Yu, 2009), possibly explaining the stronger observed relationship
21 to SOI (Table 2). Although not a focus of the current study, the greatest expression of 2.5-7
22 year periodicity occurs from the eighteenth century (Figure 2c and d), broadly coincident
23 with the end of the Northern Hemisphere Little Ice Age (LIA) chronozone (Mann et al.,
24 2009). Previous work has suggested the LIA was characterised by more pervasive ENSO
25 activity in the tropical Pacific (Cook et al., 2004; Lorrey et al., 2014; Turney and Palmer,
26 2007), suggesting the increased expression of ENSO after CE 1700 in the New Zealand
27 kauri is as a result of strengthened tropical–mid-latitude teleconnections (Li et al., 2013).
28 Curiously, we also observe significant multidecadal changes in tree growth (32-64 years)
29 prior to CE 1700 i.e. before ENSO is more strongly expressed in the kauri record (Figure
30 2C). Whether this switch in periodicities in the kauri marks a shift in the dominance of
31 different climate modes over northern New Zealand from IPO and/or SAM-like variability
32 to ENSO remains to be fully explored (Carré et al., 2014; Fowler et al., 2012; Mantua and
33 Hare, 2002; Marshall, 2003; Palmer et al., 2015b; Trouet et al., 2012).

3.2. Ancient kauri during Greenland Stadial-1 (GS-1)

The ancient kauri samples from the Towai site produced a robust chronology that spans 1,010 years with a striking downturn in growth between ~12,500 to 12,380 cal BP (Figures 2 and 6), within the period defined as GS-1 (Rasmussen et al., 2014; Steffensen et al., 2008). Although the kauri series shows other periods of below average growth, these are neither as pronounced nor as long and such a prominent downturn is unprecedented in the modern kauri record. The downturn occurred in a well-replicated portion of the chronology (Figures 2a and 6b) so it is not associated with a few spurious individuals but was instead identified in all logs buried across the site.

To investigate whether the downturn was a localized response due to a change in drainage of the basin we undertook a detailed study of the stratigraphy of the site (Figure 7). The logs spanning GS-1 fall within an upper 2-metre thick gyttja unit which is overlain by a 0.2 metre clay deposit that appears to be of Holocene age (Table 3); a further two organic rich gyttja units were observed deeper down but no logs were detected. The upper organic unit displays increasing LOI values from 30 to 70%, signifying increasing organic matter content. In the period spanning GS-1 we do observe a short-lived (approximately centennial-duration) increase in organic matter content (Figure 7), which is consistent with mid- to high-latitude studies that find wetter conditions results in an increase in carbon accumulation (Belyea and Malmer, 2004; Svensson, 1988; Turney et al., 2016a). Importantly, no-where in the sequence do we find a centennial-duration shift to minerogenic-rich sediments that might signify a major change in basin geomorphology to explain a local downturn in growth (Figure 7).

Instead, tipping point analysis detected a significant and continuously rising variance (Kendall $\tau = 0.854$, $p < 0.05$; Figure 8) prior to the downturn in tree growth at 12,500 cal. BP. This is coupled with a strong decreasing trend in autocorrelation (Kendall $\tau = -0.745$, $p < 0.05$). Relative to the null model the results are statistically significant. Both of these trends are robust to changing parameter choices, as shown by the contour plots in Figure 8c and 8d (the statistical significance is shown in the histogram plots). An increase in variance coupled with a decreasing autocorrelation is consistent with a ‘flickering’ of a climate system preceding a transition (Wang et al., 2012); however, this can be difficult to distinguish from rising variance as a result of increasing exogenous noise over time. It is necessary therefore to consider the external dynamics of the system. In this case, a composite analysis of our data suggests that a shift in the system manifested as reduced tree

1 growth is likely to have been detected, starting as early as 12,800 cal. BP. At the end of the
2 ~100 year downturn, the system abruptly recovers.

3 Importantly, the downturn in growth appears to parallel changes in the expression of
4 ENSO in the kauri tree growth (Figure 9). Prior to and during the downturn in growth we
5 observe a limited expression of ENSO periodicities in the band 2-4 years (Kestin et al.,
6 1998). After the recovery of growth ~12,380 cal. BP, however, the 2-4 year periodicity (and
7 the wider ENSO band of 2.5-7 years) (Tudhope et al., 2001) becomes a pervasive feature of
8 the kauri chronology. Tropical marine studies (Koutavas and Joanides, 2012; Leduc et al.,
9 2009; Sadekov et al., 2013) have suggested the last glacial period was characterised by
10 ‘modern’ ENSO-like activity. Whilst the southward migration in the Intertropical
11 Convergence Zone (ITCZ) has led to an increasing flow of warm northerly air masses over
12 New Zealand during the mid to late Holocene (Putnam et al., 2012), modeling studies (Liu
13 et al., 2014) appear to show similar teleconnections between the tropical Pacific and New
14 Zealand across the last glacial period. It therefore seems likely that this recovery in ENSO-
15 like periodicities in the Towai record is due to internal system dynamics, which is likely to
16 be linked to the resumption of an El Niño regime (as suggested by appearance of ENSO-like
17 periodicities in the wavelet plot, Figure 9e). Our findings are consistent with the recent
18 hypothesis that highly connected systems are more susceptible to unstable tipping points
19 (Cai et al., 2016; Praetorius and Mix, 2014).

20 *3.3. A Pacific-wide centennial duration climate change during GS-1 and possible causes*

21 The major downturn seen in the floating kauri chronology during GS-1 does not appear
22 to have been a locally induced response (Figure 7) so we compared our record to other sub-
23 decadal-resolved datasets spanning this period. Initial screening of ice core records from
24 Greenland (Rasmussen et al., 2014) or West Antarctica (WAIS Divide Project Members,
25 2015; Figure 9A and G respectively) showed no obvious downturn in the comparable time
26 period. Even allowing for sub-centennial offsets in the different chronologies (Buizert et
27 al., 2015) the ice core records can be precisely aligned via ¹⁰Be from terrestrial-ice (Adolphi
28 and Muscheler, 2016; Adolphi et al., 2014; Muscheler et al., 2014). The lack of any
29 discernable associated change in either the Greenland or Antarctic records implies nothing
30 similar is occurring in either the Atlantic or polar regions.

31 Few records exist for understanding changes in ENSO across GS-1. A 35-75 year signal
32 is observed in Pallcacocha, Ecuador (Rodbell et al., 1999), comparable to IPO and SAM

1 periodicities observed in the modern and sub-fossil kauri, and consistent with a tropical
2 Pacific signal (Figure 9E). However, limited expression of 2-4 year periodicities have been
3 reported for key timeslices in the Lateglacial part of the record, including across GS-1. In
4 the Pacific Ocean, the few available annually-resolved records that span the same period
5 appear to demonstrate a coherent pattern of change as that preserved in the Towai kauri. A
6 coral isotope record from Espiritu Santo (Corrège et al., 2004) preserves a record of SSTs
7 that shows cooler than present day temperatures. Importantly, the dating of the coral series
8 was based on 13 uranium-series ages and over 346 AMS radiocarbon age determinations
9 (Burr et al., 1998). Within the uncertainties of the U-series age control (± 21.5 years before
10 and ± 23.5 years at 1σ around hiatus), we shifted the coral sequence by 50 years to precisely
11 align against the kauri ^{14}C and find the coral preserves a sustained increase in SSTs across
12 the time of kauri downturn, immediately followed by a hiatus of coral growth (Figure 9C).
13 Corrège et al. (2004) suggest that the inferred warming at this time could have reflected the
14 southern expansion of the then reduced western Pacific warm pool. This expansion may
15 have supported conditions favorable to the expression of ENSO variability, reflected by the
16 expression of 2-4 year periodicities after $\sim 12,380$ cal. BP. Coral bleaching and mortality is
17 related to ENSO events (Eakin et al., 2009), and the re-establishment of ENSO after the
18 kauri downturn is a good candidate to explain the subsequent coral growth hiatus. Our
19 results are supported by the alignment of atmospheric (kauri) ages and coral ^{14}C after the
20 kauri climatic downturn (i.e. reduced marine radiocarbon reservoir ages) (Figure 9B),
21 consistent with stronger/more frequent ENSO events which are known to reduce
22 older/cooler upwelled water in the southeast and central Pacific (Hua et al., 2015).

23 Further south, three subfossil huon pine logs (*Lagarostrobos franklinii*) from Tasmania
24 have been reported across GS-1 (Hua et al., 2009). Importantly, however, their ring-widths
25 do not crossdate to one another despite overlapping radiocarbon ages. Similarly to the
26 Espiritu Santo coral, we were able to undertake high-precision alignment of the huon pine
27 ^{14}C series against the newly refined kauri calibration series (Hogg et al., 2016). We find that
28 the radiocarbon series of one of these huon logs (identified as SRT-779) significantly aligns
29 to the kauri ^{14}C series (agreement index $>100\%$) while the other two trees (SRT-781 and -
30 783) fail to fit (each with an agreement index of $<2\%$). The poor fit of the other two logs
31 may help explain why their ring-widths also failed to crossdate. Lensing of growth may
32 have resulted in these other huon samples missing rings in their 'consecutive' decadal
33 blocks of wood for radiocarbon dating but further study is needed to help resolve the cause.

Plotting the ring-widths of SRT779 against the Towai kauri and the Espiritu Santo coral we find a remarkably similar pattern to the downturn in growth that parallels the downturn observed in New Zealand (Figure 9D and F). The fact that this evidence from Tasmania is only from a single tree means the similar growth downturn to that observed in northern New Zealand (~2,400 kilometres apart) must be interpreted cautiously but is consistent with modern observations of enhanced southerly airflow during warming of the equatorial Pacific (Figure 4D). The result does however highlight the need for further collections of subfossil huon.

The origin of this centennial duration event remains unclear. The downturn in kauri growth (and the associated increased flickering of the climate system detected by tipping point analysis from 12,800 cal. BP) coincides with a sustained period of increased $\Delta^{14}\text{C}$ (Figure 9B and D), suggesting a possible solar role in climate forcing (Adolphi et al., 2014; Hogg et al., 2016). A previous study looking at possible drivers of tropical climate variability using the Zebiak-Cane model (Clement et al., 2001) has suggested orbital (insolation) forcing can modulate ENSO behavior. Here orbital forcing around 12 cal. (model) BP produced an ENSO that was irregular and prone to periods when variability was shut down for centuries. The associated mean state was La Nina-like, because of the absence of warm ENSO events. While $\Delta^{14}\text{C}$ is not a measure of orbital forcing *per se*, the inferred reduction in solar output (leading to elevated ^{14}C concentration in the atmosphere) may indeed have played a role in ENSO dynamics across the termination of the last glacial and into the Holocene (Marchitto et al., 2010). Crucially, the reduction in $\Delta^{14}\text{C}$ was paralleled by an increased and pervasive expression of ENSO in New Zealand kauri suggesting the establishment of different ocean-atmosphere dynamics after 12,380 cal. BP (but within GS-1) (Edwards et al., 1993).

4. Conclusions

The extent to which the return to glacial-like conditions in the North Atlantic during Greenland Stadial-1 was experienced globally remains highly uncertain. A major constraint is the absence of climate-sensitive, high-resolution (annually-resolved) records that are precisely dated from different regions of the world. Here we report a 1,010 year-long kauri (*Agathis australis*) record from northern New Zealand that has been precisely dated using comprehensive ^{14}C dating. This tropical Pacific-sensitive record preserves a striking downturn between ~12,500 to 12,380 cal. BP, firmly within GS-1. Comparison to other

1 low- and mid-latitude Pacific records with sufficient density of radiocarbon ages for high-
2 precision alignment to the kauri ^{14}C dataset suggests coherent changes in ENSO and mid-
3 latitude Southern Hemisphere westerly airflow across this period. A full understanding of
4 the drivers for this climate event remains unclear but one possibility are solar changes that
5 subsequently led to establishment and/or increased expression of central Pacific ENSO
6 across the mid-latitudes of the Pacific, seemingly independent of the Atlantic and polar
7 regions.

8 **Acknowledgements**

9 We thank Mr Alan Crawford who owns Towai Farm for access to the site and Mr Nelson
10 Parker for providing the kauri wood samples. Support was provided by the Australian
11 Research Council (grants FL100100195, LP120100310 and DP130104156), the UK Natural
12 Environment Research Council (grants NE/H009922/1 and NE/I007660/1) and GH was
13 supported by Eva-Mayr-Stihl Foundation, Waiblingen, Germany, Deutsche
14 Forschungsgemeinschaft DFG (HE3089/9-1) and the Federal Ministry of Education and
15 Research (01DR12097). Lamont-Doherty Earth Observatory contribution number XXXX.
16 We also wish to thank Dr Gretel Boswijk for an assessment of the Towai tree-ring
17 measurements and Dr Andrew Lorrey for his comments on an earlier version of the
18 manuscript.

1 Tables and Figures

2 **Table 1:** Summary details of the modern kauri tree-ring chronology and the subfossil Towai
3 chronology.

Parameter	Modern kauri master	Towai subfossil site
Number of sites	15	1
Total number of trees/series	200/428	37/92
Mean series length \pm standard deviation	211 \pm 83	517 \pm 241
Mean ring-width (mm)	1.41	1.10
Number of trees needed for an EPS>0.85	21	9
Span of years (entire)	734	1451
Span of years (EPS>0.85)	452	1010
Time interval (EPS>0.85)	CE 1550-2002	12959-11949 calBP
All series <i>rbar</i>	0.213 \pm 0.128	0.401 \pm 0.168
Within-trees <i>rbar</i>	0.490 \pm 0.069	0.770 \pm 0.128
Between-trees <i>rbar</i>	0.207 \pm 0.122	0.390 \pm 0.157

4

5 Key:

6 EPS Expressed Population Signal (Wigley et al., 1984).

7 *rbar* The average pairwise correlation between series (Cook and Kairiukstis, 1990).

Table 2: Comparison of the modern kauri chronology to three different forms of El Niño – Southern Oscillation (ENSO) records and the Southern Annular Mode (SAM) for split calibration and validation testing. The austral year starting in winter (June) and ending in autumn (May) was used for each climate variable. All models except for the SAM successfully calibrated and validated, with the SOI index producing the strongest results.

Calibration Period			Validation Period Tests			
SOI						
Model	FY – LY	RSQ	FY – LY	RSQ	RE	CE
Early	1867 – 1934	0.175	1935 – 2002	0.231	0.239	0.208
Late	1935 – 2002	0.234	1867 – 1934	0.174	0.183	0.151
TPI						
Early	1871 – 1936	0.110	1937 – 2002	0.181	0.141	0.118
Late	1937 – 2002	0.181	1871 – 1936	0.111	0.061	0.036
Niño 3.4						
Early	1857 – 1930	0.094	1931 – 2002	0.125	0.107	0.107
Late	1931 – 2002	0.124	1857 – 1930	0.093	0.067	0.062
SAM						
Early	1957 – 1989	0.006	1990 – 2002	ns	ns	ns
Late	1971-2002	0.031	1957 – 1970	ns	ns	ns

Key:

SOI	Southern Oscillation Index (Ropelewski and Jones, 1987)
TPI	TriPole Index of the Interdecadal Pacific Oscillation (IPO) (Henley et al., 2015)
Niño 3.4	Niño 3.4 sea-surface temperatures, HadISST (Rayner et al., 2003)
SAM	Southern Annular Mode (Marshall, 2003)
FY	First or initial year of calibration/verification
LY	Last or final year of calibration/verification
RSQ	Calibration or verification squared Pearson correlation
RE	Reduction of Error statistic
CE	Coefficient of Efficiency test
ns	Not significant.

Table 3: Radiocarbon ages from the Towai sedimentary sequence, calibrated using deposition modeling option in OxCal 4.2 with SHCal13 dataset (Bronk Ramsey and Lee, 2013; Hogg et al., 2013). Ages in italics did not contribute to the final age model.

Depth, cm	Laboratory number	Material	^{14}C BP $\pm 1\sigma$	Mean cal. years BP $\pm 1\sigma$
<i>10-20</i>	<i>OxA-26383</i>	<i>Bulk peat</i>	<i>1795\pm25</i>	
<i>10-20</i>	<i>OxA-26396</i>	<i>Wood</i>	<i>6017\pm36</i>	
<i>25-30</i>	<i>Wk-35470</i>	<i>Bulk peat</i>	<i>2911\pm25</i>	
<i>25-30</i>	<i>Wk-35471</i>	<i>Bulk peat</i>	<i>2273\pm25</i>	
53-54	Wk-36543	Bulk peat	8222 \pm 34	9190 \pm 70
96-97	Wk-36544	Bulk peat	9314 \pm 39	10,510 \pm 110
146-147	Wk-36545	Bulk peat	7384 \pm 33	11,840 \pm 840
181-182	Wk-39362	Bulk peat	11,920 \pm 54	13,740 \pm 150
210-211	Wk-39363	Bulk peat	13,804 \pm 62	16,700 \pm 180
273-274	Wk-39364	Bulk peat	22,204 \pm 146	26,460 \pm 270
322-323	Wk-39365	Bulk peat	36,027 \pm 814	40,470 \pm 830
<i>400-401</i>	<i>OxA-26384</i>	<i>Bulk peat</i> <i>(humic)</i>	<i>41,000\pm700</i>	
<i>400-401</i>	<i>OxA-26397</i>	<i>Bulk peat</i> <i>(humin)</i>	<i>>47,200</i>	

Figure 1: Location of ancient kauri site Towai Farm (Northland, New Zealand; filled circle), key sites discussed in text (open circles) and contoured regressions against deseasonalised and detrended contoured regressions between modern kauri tree-ring chronology and September-February sea surface temperature (HadISST; CE 1870-2002) (Rayner et al., 2003). El Niño zones are shown with black rectangles. Scale on right hand side in each panel: °C per unit of ring width. Significance $p_{\text{field}} < 0.05\%$. Analyses were made with KNMI Climate Explorer (van Oldenborgh and Burgers, 2005).

Figure 2: Modern kauri tree-ring chronology (Panel A.) with number of series contributing to the production of the tree-ring chronology (shaded histogram) and plot of the running 50-year mean of the expressed population signal (EPS) (Panel B.). Vertical line in both panels indicates the year at which an adequate sample number of trees is reached giving an EPS > 0.85 (Wigley et al., 1984); prior to this the record is potentially unreliable. The wavelet pattern of the kauri chronology since CE 1450 (Panel C.); significance level 0.90; cone of influence is shown by the white shaded area. Gaussian bandpass filtered kauri at 2.5-7 years (Tudhope et al., 2001) with Analyseries 2.0.4.2 (Paillard et al., 1996) (Panel D.).

Figure 3: Time-span and correlations of individual Towai subfossil kauri tree-ring series (Panel A.) and timing of mortality events (Panel B.). A 100-year correlation window (lagged by 50 years) is serially calculated between each tree-ring series and a master chronology built from all the other series (leave-one-out principle). Green segments are those that do not overlap completely with the width of the 100-year bin; blue segments are those that exceed $p = 0.05$. No series correlate below the critical value (Bunn, 2008). The gray column in both panels denotes the timing of the centennial-duration downturn in tree-ring growth. Note that for three trees the exact year of death was not possible to be determined because the outside portion of the log was missing or had deteriorated. Uncertainties with exact ring counts due to growth lensing and/or poorly defined ring boundaries meant the death point of the other 34 trees were binned into 100-year intervals.

Figure 4: Deseasonalised and detrended contoured regressions between modern kauri tree-ring and September-February 850 hPa height (Panel A.) and meridional wind stress (Panel B.) using 20CR 2c (HadISST; CE 1851-2002) (Compo et al., 2011). Also shown are the lagged 2 month response of kauri growth to September-February 850 hPa height (Panel C.) and meridional wind stress (Panel D.) Scale on right hand side in each panel: hPa and ms^{-1}

per unit of ring width respectively. Significance $p_{\text{field}} < 0.05\%$. Analyses were made with KNMI Climate Explorer (van Oldenborgh and Burgers, 2005).

Figure 5: Correlations and significance between the modern kauri tree-ring indices and the Southern Oscillation Index (SOI) stratified by different phases of the Interdecadal Pacific Oscillation (IPO) (approach modified from Table 1 of Power et al., 1999).

Figure 6: Towai subfossil kauri tree-ring chronology (Panel A.) with number of series contributing to the production of the tree-ring chronology (shaded histogram) and plot of the running 50-year mean of the expressed population signal (EPS) (Panel B.). Vertical lines in both panels indicate the years at which an adequate sample number of trees are reached giving an $\text{EPS} > 0.85$ (Wigley et al., 1984); either side of this the record is potentially unreliable.

Figure 7: Lithostratigraphy at Towai Farm, with age-depth model (derived using OxCal 4.2 and SHCal13) (Bronk Ramsey and Lee, 2013; Hogg et al., 2013) and loss-on-ignition (LOI). Grey shaded area defines modelled stratigraphic position of the Greenland Stadial-1 (GS-1) chronozone (12.9-11.65 ka BP) (Hogg et al., 2016; Rasmussen et al., 2014). The identified centennial-duration peak in LOI indicates enhanced organic matter content of the sediments, possibly as a result of a wetter phase in the basin and coincident with the kauri downturn.

Figure 8: Tipping point analysis of Towai chronology. Towai chronology with Gaussian-kernel smoothing filter shown (purple line) (Panel a). Residuals from the detrended data (Panel b). Autocorrelation over the sliding window (window = 50% of data) (Panel c). Variance over the sliding window (Panel d). Kendall τ values indicate the statistical strength of the trend. The inset contour plots (left) in c) and d) indicate the sensitivity of the analysis to the size of the sliding window and detrending bandwidth. The inset histograms (right) in c) and d) indicate the significance of the analysis using surrogate time series.

Figure 9: Comparison between the Towai kauri series and key datasets spanning the GS-1 chronozone: North Greenland $\delta^{18}\text{O}$ on the GICC05 timescale relative to CE 1950 (Steffensen et al., 2008) (Panel A.); $\Delta^{14}\text{C}$ in Towai ancient kauri (solid symbols) (Hogg et al., 2016), reservoir-corrected Espiritu Santo coral (solid red symbols) (Burr et al., 1998) and Tasmanian huon pine (solid orange symbols) (Hua et al., 2009) (B.); reconstructed sea surface temperatures (SSTs) from Espiritu Santo (Corrège et al., 2004) (C.); Towai standardised

1 kauri tree-ring index (solid black with dashed white line for mean) (D.), wavelet pattern
2 (significance level 0.90; solid white line denotes cone of influence) (E.) and Gaussian
3 bandpass filtered kauri at 2.5-7 years (Tudhope et al., 2001) with Analyseries 2.0.4.2
4 (Paillard et al., 1996) (F.); Huon pine tree (SRT-779) tree ring measurements (orange line)
5 (Hua et al., 2009) (G.); and West Antarctic Ice Sheet $\delta^{18}\text{O}$ (WAIS Divide Project Members,
6 2015) (Panel H.). Onset of increased atmospheric $\Delta^{14}\text{C}$ given by vertical dashed line
7 coinciding with increased ‘flickering’ in kauri tree-ring series; grey column marks centennial-
8 duration climate event. Termination of the Antarctic Cold Reversal (ACR) as inferred by the
9 stepped increase in the interhemispheric ^{14}C gradient (Hogg et al., 2016).

References

- Adolphi, F., Muscheler, R., 2016. Synchronizing the Greenland ice core and radiocarbon timescales over the Holocene—Bayesian wiggle-matching of cosmogenic radionuclide records. *Climate of the Past* 12, 15-30.
- Adolphi, F., Muscheler, R., Svensson, A., Aldahan, A., Possnert, G., Beer, J., Sjolte, J., Bjorck, S., Matthes, K., Thieblemont, R., 2014. Persistent link between solar activity and Greenland climate during the Last Glacial Maximum. *Nature Geoscience* 7, 662-666.
- Baker, P.J., Palmer, J.G., D'Arrigo, R., 2008. The dendrochronology of *Callitris intratropica* in northern Australia: annual ring structure, chronology development and climate correlations. *Australian Journal of Botany* 56, 311-320.
- Barrell, D.J., Almond, P.C., Vandergoes, M.J., Lowe, D.J., Newnham, R.M., members, I., 2013. A composite pollen-based stratotype for inter-regional evaluation of climatic events in New Zealand over the past 30,000 years (NZ-INTIMATE project). *Quaternary Science Reviews* 74, 4-20.
- Bartolomé, M., Moreno, A., Sancho, C., Stoll, H.M., Cacho, I., Spötl, C., Belmonte, Á., Edwards, R.L., Cheng, H., Hellstrom, J.C., 2015. Hydrological change in Southern Europe responding to increasing North Atlantic overturning during Greenland Stadial 1. *Proceedings of the National Academy of Sciences* 112, 6568-6572.
- Belyea, L.R., Malmer, N., 2004. Carbon sequestration in peatland: patterns and mechanisms of response to climate change. *Global Change Biology* 10, 1043-1052.
- Björck, S., Kromer, B., Johnsen, S., Bennike, O., Hammarlund, D., Lemdahl, G., Possnert, G., Rasmussen, T.L., Wohlfarth, B., Hammer, C.U., Spurk, M., 1996. Synchronized terrestrial atmospheric deglacial records around the North Atlantic. *Science* 274, 1155-1160.
- Blockley, S.P.E., Lane, C.S., Hardiman, M., Rasmussen, S.O., Seierstad, I.K., Steffensen, J.P., Svensson, A., Lotter, A.F., Turney, C.S.M., Bronk Ramsey, C., INTIMATE members, 2012. Synchronisation of palaeoenvironmental records over the last 60,000 years, and an extended INTIMATE event stratigraphy to 48,000 b2k. *Quaternary Science Reviews* 36, 2-10.
- Boswijk, G., Fowler, A., Lorrey, A., Palmer, J., Ogden, J., 2006. Extension of the New Zealand kauri (*Agathis australis*) chronology to 1724 BC. *The Holocene* 16, 188-199.
- Boswijk, G., Fowler, A.M., Palmer, J.G., Fenwick, P., Hogg, A., Lorrey, A., Wunder, J., 2014. The late Holocene kauri chronology: assessing the potential of a 4500-year record for palaeoclimate reconstruction. *Quaternary Science Reviews* 90, 128-142.

- 1 Brauer, A., Endres, C., Günter, C., Litt, T., Stebich, M., Negendank, J.F., 1999. High
2 resolution sediment and vegetation responses to Younger Dryas climate change in varved
3 lake sediments from Meerfelder Maar, Germany. *Quaternary Science Reviews* 18, 321-
4 329.
- 5 Brien, R.J., Schöngart, J., Zuidema, P.A., 2016. Tree rings in the tropics: Insights into the
6 ecology and climate sensitivity of tropical trees, *Tropical Tree Physiology*. Springer, pp.
7 439-461.
- 8 Broecker, W.S., 1997. Thermohaline circulation, the Achilles Heel of our climate system:
9 will man-made CO₂ upset the current balance? *Science* 278, 1582-1588.
- 10 Bronk Ramsey, C., 2008. Radiocarbon dating: revolutions in understanding. *Archaeometry*
11 50, 249-275.
- 12 Bronk Ramsey, C., 2011. Dealing with outliers and offsets in radiocarbon dating.
13 *Radiocarbon* 51, 1023-1045.
- 14 Bronk Ramsey, C., Higham, T., Leach, P., 2004. Towards high-precision AMS; progress and
15 limitations. *Radiocarbon* 46, 17-24.
- 16 Bronk Ramsey, C., Lee, S., 2013. Recent and planned developments of the program OxCal.
17 *Radiocarbon* 55, 720-730.
- 18 Bronk Ramsey, C., Staff, R.A., Bryant, C.L., Brock, F., Kitagawa, H., van der Plicht, J.,
19 Schlögl, G., Marshall, M.H., Brauer, A., Lamb, H.F., Payne, R.L., Tarasov, P.E.,
20 Haraguchi, T., Gotanda, K., Yonenobu, H., Yokoyama, Y., Tada, R., Nakagawa, T., 2012.
21 A complete terrestrial radiocarbon record for 11.2 to 52.8 kyr B.P. *Science* 338, 370-374.
- 22 Buckley, B., Ogden, J., Palmer, J., Fowler, A.M., Salinger, J., 2000. Dendroclimatic
23 interpretation of tree-rings in *Agathis australis* (kauri). 1. Climate correlation functions
24 and master chronology. *Journal of the Royal Society of New Zealand* 30, 263-275.
- 25 Buckley, B.M., Anchukaitis, K.J., Penny, D., Fletcher, R., Cook, E.R., Sano, M., Le, C.N.,
26 Wichienkeo, A., Ton, T.M., Truong, M.H., 2010. Climate as a contributing factor in the
27 demise of Angkor, Cambodia. *Proceedings of the National Academy of Sciences of the*
28 *United States of America* 107, 6748-6752.
- 29 Buizert, C., Cuffey, K.M., Severinghaus, J.P., Baggenstos, D., Fudge, T.J., Steig, E.J.,
30 Markle, B.R., Winstrup, M., Rhodes, R.H., Brook, E.J., Sowers, T.A., Clow, G.D., Cheng,
31 H., Edwards, R.L., Sigl, M., McConnell, J.R., Taylor, K.C., 2015. The WAIS Divide deep
32 ice core WD2014 chronology; Part 1: Methane synchronization (68–31 ka BP) and the gas
33 age–ice age difference. *Climates of the Past* 11, 153-173.

- 1 Bunn, A.G., 2008. A dendrochronology program library in R (dplR). *Dendrochronologia* 26,
2 115-124.
- 3 Burr, G.S., Beck, J.W., Taylor, F.W., Récy, J., Edwards, R.L., Cabioch, G., Corrège, T.,
4 Donahue, D.J., O'Malley, J.M., 1998. A high-resolution radiocarbon calibration between
5 11,700 and 12,400 calendar years BP derived from ^{230}Th ages of corals from Espiritu
6 Santo Island, Vanuatu. *Radiocarbon* 40, 1093-1105.
- 7 Cai, W., Cowan, T., Thatcher, M., 2012. Rainfall reductions over Southern Hemisphere semi-
8 arid regions: the role of subtropical dry zone expansion. *Scientific Reports* 2, 702.
- 9 Cai, Y., Lenton, T.M., Lontzek, T.S., 2016. Risk of multiple interacting tipping points should
10 encourage rapid CO₂ emission reduction. *Nature Clim. Change* 6, 520-525.
- 11 Carlson, A.E., Clark, P.U., 2012. Ice sheet sources of sea level rise and freshwater discharge
12 during the last deglaciation. *Reviews of Geophysics* 50, RG4007.
- 13 Carlson, A.E., Clark, P.U., Haley, B.A., Klinkhammer, G.P., Simmons, K., Brook, E.J.,
14 Meissner, K.J., 2007. Geochemical proxies of North American freshwater routing during
15 the Younger Dryas cold event. *Proceedings of the National Academy of Sciences* 104,
16 6556-6561.
- 17 Carpenter, S., Brock, W., 2006. Rising variance: a leading indicator of ecological transition.
18 *Ecology letters* 9, 311-318.
- 19 Carré, M., Sachs, J.P., Purca, S., Schauer, A.J., Braconnot, P., Falcón, R.A., Julien, M.,
20 Lavallée, D., 2014. Holocene history of ENSO variance and asymmetry in the eastern
21 tropical Pacific. *Science* 345, 1045-1048.
- 22 Clement, A.C., Cane, M.A., Seager, R., 2001. An orbitally driven tropical source for abrupt
23 climate change. *Journal of Climate* 14, 2369-2375.
- 24 Collins, M., An, S.-I., Cai, W., Ganachaud, A., Guilyardi, E., Jin, F.-F., Jochum, M.,
25 Lengaigne, M., Power, S., Timmermann, A., Vecchi, G., Wittenberg, A., 2010. The
26 impact of global warming on the tropical Pacific Ocean and El Niño. *Nature Geoscience* 3,
27 391-397.
- 28 Compo, G.P., Whitaker, J.S., Sardeshmukh, P.D., Matsui, N., Allan, R.J., Yin, X., Gleason,
29 B.E., Vose, R.S., Rutledge, G., Bessemoulin, P., Brönnimann, S., Brunet, M., Crouthamel,
30 R.I., Grant, A.N., Groisman, P.Y., Jones, P.D., Kruk, M.C., Kruger, A.C., Marshall, G.J.,
31 Maugeri, M., Mok, H.Y., Nordli, Ø., Ross, T.F., Trigo, R.M., Wang, X.L., Woodruff, S.D.,
32 Worley, S.J., 2011. The Twentieth Century Reanalysis Project. *Quarterly Journal of the*
33 *Royal Meteorological Society* 137, 1-28.

- 1 Cook, E.R., 1985. A Time Series Approach to Tree-Ring Standardization. University of
2 Arizona, Tucson, Arizona, USA.
- 3 Cook, E.R., Kairiukstis, L.A., 1990. Methods of dendrochronology: Applications in the
4 environmental sciences. Kluwer Academic Publishers, Dordrecht, Netherlands.
- 5 Cook, E.R., Peters, K., 1997. Calculating unbiased tree-ring indices for the study of climatic
6 and environmental change. *The Holocene* 7, 361-370.
- 7 Cook, E.R., Woodhouse, C.A., Eakin, C.M., Meko, D.M., Stahle, D.W., 2004. Long-term
8 aridity changes in the western United States. *Science* 306, 1015-1018.
- 9 Cooper, A., Turney, C., Hughen, K.A., Brook, B.W., McDonald, H.G., Bradshaw, C.J.A.,
10 2015. Abrupt warming events drove Late Pleistocene Holarctic megafaunal turnover.
11 *Science* 349, 602-606.
- 12 Corrège, T., Gagan, M.K., Beck, J.W., Burr, G.S., Cabioch, G., Le Cornec, F., 2004.
13 Interdecadal variation in the extent of South Pacific tropical waters during the Younger
14 Dryas event. *Nature* 428, 927-929.
- 15 Cram, T.A., Compo, G.P., Yin, X., Allan, R.J., McColl, C., Vose, R.S., Whitaker, J.S.,
16 Matsui, N., Ashcroft, L., Auchmann, R., 2015. The International Surface Pressure
17 Databank version 2. *Geoscience Data Journal* 2, 31-46.
- 18 Dakos, V., Carpenter, S.R., Brock, W.A., Ellison, A.M., Guttal, V., Ives, A.R., Kefi, S.,
19 Livina, V., Seekell, D.A., van Nes, E.H., 2012. Methods for detecting early warnings of
20 critical transitions in time series illustrated using simulated ecological data. *PloS One* 7,
21 e41010.
- 22 Dakos, V., Scheffer, M., van Nes, E.H., Brovkin, V., Petoukhov, V., Held, H., 2008. Slowing
23 down as an early warning signal for abrupt climate change. *Proceedings of the National*
24 *Academy of Sciences* 105, 14308-14312.
- 25 Dee, M., Ramsey, C.B., 2000. Refinement of graphite target production at ORAU. *Nuclear*
26 *Instruments and Methods in Physics Research Section B: Beam Interactions with*
27 *Materials and Atoms* 172, 449-453.
- 28 Doughty, A.M., Anderson, B.M., Mackintosh, A.N., Kaplan, M.R., Vandergoes, M.J., Barrell,
29 D.J.A., Denton, G.H., Schaefer, J.M., Chinn, T.J.H., Putnam, A.E., 2013. Evaluation of
30 Lateglacial temperatures in the Southern Alps of New Zealand based on glacier modelling
31 at Irishman Stream, Ben Ohau Range. *Quaternary Science Reviews* 74, 160-169.
- 32 Eakin, C.M., Lough, J.M., Heron, S.F., 2009. Climate Variability and Change: Monitoring
33 Data and Evidence for Increased Coral Bleaching Stress, in: van Oppen, M.J.H., Lough,

- J.M. (Eds.), Coral Bleaching: Patterns, Processes, Causes and Consequences. Springer Berlin Heidelberg, Berlin, Heidelberg, pp. 41-67.
- Edwards, R.L., Beck, J.W., Burr, G.S., Donahue, D.J., Chappell, J.M.A., Bloom, A.L., Druffel, E.R.M., Taylor, F.W., 1993. A large drop in atmospheric $^{14}\text{C}/^{12}\text{C}$ and reduced melting in the Younger Dryas, documented with ^{230}Th ages of corals. *Science* 260, 962-968.
- EPICA Community Members, 2006. One-to-one coupling of glacial climate variability in Greenland and Antarctica. *Nature* 444, 195-198.
- Fowler, A.M., 2008. ENSO history recorded in *Agathis australis* (kauri) tree rings. Part B: 423 years of ENSO robustness. *International Journal of Climatology* 28, 21–35.
- Fowler, A., Palmer, J., Salinger, J., Ogden, J., 2000. Dendroclimatic interpretation of tree-rings in *Agathis australis* (kauri): 2. Evidence of a significant relationship with ENSO. *Journal of the Royal Society of New Zealand* 30, 277-292.
- Fowler, A.M., Boswijk, G., Lorrey, A.M., Gergis, J., Pirie, M., McCloskey, S.P.J., Palmer, J.G., Wunder, J., 2012. Multi-centennial tree-ring record of ENSO-related activity in New Zealand. *Nature Climate Change* 2, 172-176.
- Fowler, A.M., Boswijk, G., Ogden, J., 2004. Tree-ring studies on *Agathis australis* (kauri): A synthesis of development work on late Holocene chronologies. *Tree-Ring Research* 60, 15-29.
- Fowler, A.M., Gretel, B., Gergis, J., Lorrey, A., 2008. ENSO history recorded in *Agathis australis* (kauri) tree rings. Part A: Kauri's potential as an ENSO proxy. *International Journal of Climatology*, 1-20.
- Gordon, N.D., 1985. The Southern Oscillation: a New Zealand perspective. *Journal of the Royal Society of New Zealand* 15, 137-155.
- Gouhier, T.C., Grinstead, A., Simko, V., 2016. biwavelet: Conduct univariate and bivariate wavelet analyses (Version 0.20.7). Available from <http://github.com/tgouhier/biwavelet>
- Grissino-Mayer, H.D., 2001. Evaluating crossdating accuracy: A manual and tutorial for the computer program COFECHA. *Tree-Ring Research* 57, 205-221.
- Held, H., Kleinen, T., 2004. Detection of climate system bifurcations by degenerate fingerprinting. *Geophysical Research Letters* 31, doi: 10.1029/2004GL020972.
- Henley, B.J., Gergis, J., Karoly, D.J., Power, S., Kennedy, J., Folland, C.K., 2015. A tripole index for the Interdecadal Pacific Oscillation. *Climate Dynamics* 45, 3077-3090.
- Hogg, A., Southon, J., Turney, C., Palmer, J., Bronk Ramsey, C., Fenwick, P., Boswijk, G., Friedrich, M., Helle, G., Hughen, K., Jones, R., Kromer, B., Noronha, A., Reynard, L.,

- Staff, R., Wacker, L., 2016. Punctuated shutdown of Atlantic Meridional Overturning Circulation during the Greenland Stadial 1. *Scientific Reports* 6, 25902, doi: 25910.21038/srep25902.
- Hogg, A.G., Fifield, L.K., Turney, C.S.M., Palmer, J.G., Galbraith, R., M., B., 2006. Dating ancient wood by high sensitivity Liquid Scintillation Spectroscopy and Accelerator Mass Spectrometry - Pushing the boundaries. *Quaternary Geochronology* 1, 241-248.
- Hogg, A.G., Hua, Q., Blackwell, P.G., Niu, M., Buck, C.E., Guilderson, T.P., Heaton, T.J., Palmer, J.G., Reimer, P.J., Reimer, R.W., Turney, C.S.M., Zimmerman, S.R.H., 2013. SHCal13 Southern Hemisphere calibration, 0–50,000 years cal BP. *Radiocarbon* 55, 1889-1903.
- Hua, Q., Barbetti, M., Fink, D., Kaiser, K.F., Friedrich, M., Kromer, B., Levchenko, V.A., Zoppi, U., Smith, A.M., Bertuch, F., 2009. Atmospheric ^{14}C variations derived from tree rings during the early Younger Dryas. *Quaternary Science Reviews* 28, 2982-2990.
- Hua, Q., Webb, G.E., Zhao, J.-x., Nothdurft, L.D., Lybolt, M., Price, G.J., Opdyke, B.N., 2015. Large variations in the Holocene marine radiocarbon reservoir effect reflect ocean circulation and climatic changes. *Earth and Planetary Science Letters* 422, 33-44.
- Hughen, K.A., Southon, J.R., Bertrand, C.J.H., Frantz, B., Zerbeño, P., 2004. Cariaco Basin calibration update: Revisions to calendar and ^{14}C chronologies for core PL07-58PC. *Radiocarbon* 46, 1161-1187.
- Iizumi, T., Luo, J.-J., Challinor, A.J., Sakurai, G., Yokozawa, M., Sakuma, H., Brown, M.E., Yamagata, T., 2014. Impacts of El Niño Southern Oscillation on the global yields of major crops. *Nat Commun* 5.
- Jara, I.A., Newnham, R.M., Vandergoes, M.J., Foster, C.R., Lowe, D.J., Wilmshurst, J.M., Moreno, P.I., Renwick, J.A., Homes, A.M., 2015. Pollen–climate reconstruction from northern South Island, New Zealand (41° S), reveals varying high - and low - latitude teleconnections over the last 16 000 years. *Journal of Quaternary Science* 30, 817-829.
- Jiang, N., Griffiths, G., Lorrey, A., 2013. Influence of large-scale climate modes on daily synoptic weather types over New Zealand. *International Journal of Climatology* 33, 499-519.
- Kaiser, K.F., Friedrich, M., Miramont, C., Kromer, B., Sgier, M., Schaub, M., Boeren, I., Remmele, S., Talamo, S., Guibal, F., 2012. Challenging process to make the Lateglacial tree-ring chronologies from Europe absolute—an inventory. *Quaternary Science Reviews* 36, 78-90.

1 Kao, H.-Y., Yu, J.-Y., 2009. Contrasting Eastern-Pacific and Central-Pacific Types of ENSO.
2 Journal of Climate 22, 615-632.

3 Kendall, M.G., 1948. Rank Correlation Methods. Griffen, Oxford.

4 Kershaw, A.P., 1997. A modification of the Troels-Smith system on sediment description and
5 portrayal. Quaternary Australasia 15, 63-68.

6 Kestin, T.S., Karoly, D.J., Yano, J.-I., Rayner, N.A., 1998. Time–frequency variability of
7 ENSO and stochastic simulations. Journal of Climate 11, 2258-2272.

8 Kiem, A.S., Franks, S.W., Kuczera, G., 2003. Multi-decadal variability of flood risk.
9 Geophysical Research Letters 30, n/a-n/a.

10 King, A.D., Alexander, L.V., Donat, M.G., 2013. Asymmetry in the response of eastern
11 Australia extreme rainfall to low - frequency Pacific variability. Geophysical Research
12 Letters 40, 2271-2277.

13 Kosaka, Y., Xie, S.-P., 2013. Recent global-warming hiatus tied to equatorial Pacific surface
14 cooling. Nature 501, 403-407.

15 Koutavas, A., Joanides, S., 2012. El Niño-Southern Oscillation extrema in the Holocene and
16 Last Glacial Maximum. Paleoceanography 27, PA4208.

17 Kromer, B., Friedrich, M., Hughen, K.A., Kaiser, F., Remmele, S., Schaub, M., Talamo, S.,
18 2004. Late glacial ¹⁴C ages from a floating 1382-ring pine chronology. Radiocarbon 46,
19 1203-1209.

20 Lane, C.S., Brauer, A., Blockley, S.P.E., Dulski, P., 2013. Volcanic ash reveals time-
21 transgressive abrupt climate change during the Younger Dryas. Geology 41, 1251-1254.

22 Leduc, G., Vidal, L., Cartapanis, O., Bard, E., 2009. Modes of eastern equatorial Pacific
23 thermocline variability: Implications for ENSO dynamics over the last glacial period.
24 Paleoceanography 24, n/a-n/a.

25 Lenton, T.M., Livina, V.N., Dakos, V., van Nes, E.H., Scheffer, M., 2012. Early warning of
26 climate tipping points from critical slowing down: comparing methods to improve
27 robustness. Philosophical Transactions of the Royal Society A: Mathematical, Physical
28 and Engineering Sciences 370, 1185-1204.

29 Li, J., Xie, S.-P., E.R., C., Morales, M.S., Christie, D.A., Johnson, N.C., Chen, F.-C.a.L., W.-
30 H., D'Arrigo, R., Fowler, A.M., Gou, X., Fang, K., 2013. El Niño modulations over the
31 past seven centuries. Nature Climate Change 3, 822-826.

32 Liu, Z., Lu, Z., Wen, X., Otto-Bliesner, B.L., Timmermann, A., Cobb, K.M., 2014. Evolution
33 and forcing mechanisms of El Nino over the past 21,000 years. Nature 515, 550-553.

- 1 Lorrey, A., Fauchereau, N., Stanton, C., Chappell, P., Phipps, S., Mackintosh, A., Renwick, J.,
2 Goodwin, I., Fowler, A., 2014. The Little Ice Age climate of New Zealand reconstructed
3 from Southern Alps cirque glaciers: a synoptic type approach. *Climate Dynamics* 42,
4 3039-3060.
- 5 Lorrey, A., Martin, T., 2005. Use of modern tree-fall patterns as a guideline for interpreting
6 prostrate trees at a pre-Last Glacial Maximum paleoforest site, upper North Island, New
7 Zealand. *Journal of Geophysical Research: Biogeosciences* 110, n/a-n/a.
- 8 Lowe, D.J., Blaauw, M., Hogg, A.G., Newnham, R.M., 2013. Ages of 24 widespread tephras
9 erupted since 30,000 years ago in New Zealand, with re-evaluation of the timing and
10 palaeoclimatic implications of the Lateglacial cool episode recorded at Kaipo bog.
11 *Quaternary Science Reviews* 74, 170-194.
- 12 Lowe, J.J., 2001. Abrupt climatic changes in Europe during the last glacial-interglacial
13 transition: the potential for testing hypotheses on the synchronicity of climatic events using
14 tephrochronology. *Global and Planetary Change* 30, 73-84.
- 15 Lu, J., Chen, G., Frierson, D.M., 2008. Response of the zonal mean atmospheric circulation
16 to El Niño versus global warming. *Journal of Climate* 21, 5835-5851.
- 17 Lynch-Stieglitz, J., Schmidt, M.W., Gene Henry, L., Curry, W.B., Skinner, L.C., Mulitza, S.,
18 Zhang, R., Chang, P., 2014. Muted change in Atlantic overturning circulation over some
19 glacial-aged Heinrich events. *Nature Geoscience* 7, 144-150.
- 20 MacDonald, G.M., Moser, K.A., Bloom, A.M., Porinchu, D.F., Potito, A.P., Wolfe, B.B.,
21 Edwards, T.W., Petel, A., Orme, A.R., Orme, A.J., 2008. Evidence of temperature
22 depression and hydrological variations in the eastern Sierra Nevada during the Younger
23 Dryas stage. *Quaternary Research* 70, 131-140.
- 24 Mann, M.E., Zhang, Z., Rutherford, S., Bradley, R.S., Hughes, M.K., Shindell, D., Ammann,
25 C., Faluvegi, G., Ni, F., 2009. Global signatures and dynamical origins of the Little Ice
26 Age and Medieval Climate Anomaly. *Science* 326, 1256-1260.
- 27 Mantua, N.J., Hare, S.R., 2002. The Pacific Decadal Oscillation. *Journal of Oceanography* 58,
28 35-44.
- 29 Marchitto, T.M., Muscheler, R., Ortiz, J.D., Carriquiry, J.D., van Geen, A., 2010. Dynamical
30 response of the tropical Pacific Ocean to solar forcing during the early Holocene. *Science*
31 330, 1378-1381.
- 32 Marshall, G., 2003. Trends in the Southern Annular Mode from observations and reanalyses.
33 *Journal of Climate* 16, 4134-4143.

- 1 Mayle, F.E., Bell, M., Birks, H.H., Brooks, S.J., Coope, G.R., Lowe, J.J., Sheldrick, C.,
2 Shijie, L., Turney, C.S.M., Walker, M.J.C., 1999. Climate variations in Britain during the
3 Last Glacial-Holocene transition (15.0-11.5 cal ka BP): comparison with the GRIP ice-
4 core record. *Journal of the Geological Society of London* 156, 411-423.
- 5 McGlone, M.S., Turney, C.S.M., Wilmshurst, J.M., Pahnke, K., 2010. Divergent trends in
6 land and ocean temperature in the Southern Ocean over the past 18,000 years. *Nature*
7 *Geoscience* 3, 622-626.
- 8 McPhaden, M.J., Zebiak, S.E., Glantz, M.H., 2006. ENSO as an Integrating Concept in Earth
9 Science. *Science* 314, 1740-1745.
- 10 Melvin, T.M., Briffa, K.R., 2008. A “signal-free” approach to dendroclimatic standardisation.
11 *Dendrochronologia* 26, 71-86.
- 12 Muscheler, R., Adolphi, F., Knudsen, M.F., 2014. Assessing the differences between the
13 IntCal and Greenland ice-core time scales for the last 14,000 years via the common
14 cosmogenic radionuclide variations. *Quaternary Science Reviews* 106, 81-87.
- 15 Muschitiello, F., Pausata, F.S.R., Watson, J.E., Smittenberg, R.H., Salih, A.A.M., Brooks,
16 S.J., Whitehouse, N.J., Karlatou-Charalampopoulou, A., Wohlfarth, B., 2015.
17 Fennoscandian freshwater control on Greenland hydroclimate shifts at the onset of the
18 Younger Dryas. *Nature Communications* 6, doi: 10.1038/ncomms9939.
- 19 Ogden, J., Newnham, R.M., Palmer, J.G., Serra, R.G., Mitchell, N.D., 1993. Climatic
20 implications of macro-and microfossil assemblages from Late Pleistocene deposits in
21 Northern New Zealand. *Quaternary Research* 39, 107-119.
- 22 Paillard, D., Labeyrie, L., Yiou, P., 1996. Macintosh program performs time-series analysis.
23 *Eos* 77, 379.
- 24 Palmer, J., Lorrey, A., Turney, C.S.M., Hogg, A., Baillie, M., Fifield, K., Ogden, J., 2006.
25 Extension of New Zealand kauri (*Agathis australis*) tree-ring chronologies into Oxygen
26 Isotope Stage (OIS)-3. *Journal of Quaternary Science* 21, 779-787.
- 27 Palmer, J., Ogden, J., 1983. A dendrometer band study of the seasonal pattern of radial
28 increment in kauri (*Agathis australis*). *New Zealand journal of botany* 21, 121-125.
- 29 Palmer, J., Turney, C.S.M., Hogg, A.G., Lorrey, A.M., Jones, R.J., 2015a. Progress in
30 refining the global radiocarbon calibration curve using New Zealand kauri (*Agathis*
31 *australis*) tree-ring series from Oxygen Isotope Stage 3. *Quaternary Geochronology* 27,
32 158-163.
- 33 Palmer, J.G., Cook, E.R., Turney, C.S.M., Allen, K., Fenwick, P., Cook, B.I., O'Donnell, A.,
34 Lough, J.M., Grierson, P., Baker, P., 2015b. Drought variability in the eastern Australia

and New Zealand summer drought atlas (ANZDA, CE 1500–2012) modulated by the Interdecadal Pacific Oscillation. *Environmental Research Letters* 10, 124002.

Partin, J.W., Quinn, T.M., Shen, C.C., Okumura, Y., Cardenas, M.B., Siringan, F.P., Banner, J.L., Lin, K., Hu, H.M., Taylor, F.W., 2015. Gradual onset and recovery of the Younger Dryas abrupt climate event in the tropics. *Nat Commun* 6.

Pedro, J.B., Bostock, H.C., Bitz, C.M., He, F., Vandergoes, M.J., Steig, E.J., Chase, B.M., Krause, C.E., Rasmussen, S.O., Markle, B.R., Cortese, G., 2016. The spatial extent and dynamics of the Antarctic Cold Reversal. *Nature Geosci* 9, 51-55.

Pepper, A.C., Shulmeister, J., Nobes, D.C., Augustinus, P.A., 2004. Possible ENSO signals prior to the Last Glacial Maximum, during the last deglaciation and the early Holocene, from New Zealand. *Geophysical Research Letters* 31, doi:10.1029/2004GL020236.

Power, S., Casey, T., Folland, C., Colman, A., Mehta, V., 1999. Inter-decadal modulation of the impact of ENSO on Australia. *Climate Dynamics* 15, 319-324.

Praetorius, S.K., Mix, A.C., 2014. Synchronization of North Pacific and Greenland climates preceded abrupt deglacial warming. *Science* 345, 444-448.

Putnam, A.E., Schaefer, J.M., Denton, G.H., Barrell, D.J.A., Finkel, R.C., Andersen, B.G., Schwartz, R., Chinn, T.J.H., Doughty, A.M., 2012. Regional climate control of glaciers in New Zealand and Europe during the pre-industrial Holocene. *Nature Geosci* 5, 627-630.

Rach, O., Brauer, A., Wilkes, H., Sachse, D., 2014. Delayed hydrological response to Greenland cooling at the onset of the Younger Dryas in western Europe. *Nature Geoscience* 7, 109-112.

Rasmussen, S.O., Bigler, M., Blockley, S.P., Blunier, T., Buchardt, S.L., Clausen, H.B., Cvijanovic, I., Dahl-Jensen, D., Johnsen, S.J., Fischer, H., Gkinis, V., Guillevic, M., Hoek, W.Z., Lowe, J.J., Pedro, J.B., Popp, T., Seierstad, I.K., Steffensen, J.P., Svensson, A.M., Vallelonga, P., Vinther, B.M., Walker, M.J.C., Wheatley, J.J., Winstrup, M., 2014. A stratigraphic framework for abrupt climatic changes during the Last Glacial period based on three synchronized Greenland ice-core records: refining and extending the INTIMATE event stratigraphy. *Quaternary Science Reviews* 106, 14-28.

Rayner, N.A., Parker, D.E., Horton, E.B., Folland, C.K., Alexander, L.V., Rowell, D.P., Kent, E.C., Kaplan, A., 2003. Global analyses of sea surface temperature, sea ice, and night marine air temperature since the late nineteenth century. *Journal of Geophysical Research: Atmospheres* 108, 4407, doi:10.1029/2002JD002670.

Reeves, J.M., Barrows, T.T., Cohen, T.J., Kiem, A.S., Bostock, H.C., Fitzsimmons, K.E., Jansen, J.D., Kemp, J., Krause, C., Petherick, L., Phipps, S.J., 2013. Climate variability

over the last 35,000 years recorded in marine and terrestrial archives in the Australian region: an OZ-INTIMATE compilation. *Quaternary Science Reviews* 74, 21-34.

Renssen, H., Mairesse, A., Goosse, H., Mathiot, P., Heiri, O., Roche, D.M., Nisancioglu, K.H., Valdes, P.J., 2015. Multiple causes of the Younger Dryas cold period. *Nature Geoscience* 8, 946-949.

Rodbell, D.T., Seltzer, G.O., Anderson, D.M., Abbott, M.B., Enfield, D.B., Newman, J.H., 1999. An ~15,000-year record of El Niño-driven alluviation in southwestern Ecuador. *Science* 283, 516-520.

Ropelewski, C.F., Jones, P.D., 1987. An extension of the Tahiti-Darwin Southern Oscillation Index. *Monthly Weather Review* 115, 2161-2165.

Sadekov, A.Y., Ganeshram, R., Pichevin, L., Berdin, R., McClymont, E., Elderfield, H., Tudhope, A.W., 2013. Palaeoclimate reconstructions reveal a strong link between El Niño-Southern Oscillation and Tropical Pacific mean state. *Nat Commun* 4.

Salinger, M.J., Renwick, J.A., Mullan, A.B., 2001. Interdecadal Pacific Oscillation and south Pacific climate. *International Journal of Climatology* 21, 1705-1721.

Schollaen, K., Heinrich, I., Neuwirth, B., Krusic, P.J., D'Arrigo, R.D., Karyanto, O., Helle, G., 2013. Multiple tree-ring chronologies (ring width, $\delta^{13}\text{C}$ and $\delta^{18}\text{O}$) reveal dry and rainy season signals of rainfall in Indonesia. *Quaternary Science Reviews* 73, 170-181.

Southon, J., Noronha, A.L., Cheng, H., Edwards, R.L., Wang, Y., 2012. A high-resolution record of atmospheric ^{14}C based on Hulu Cave speleothem H82. *Quaternary Science Reviews* 33, 32-41.

Steffensen, J.P., Andersen, K.K., Bigler, M., Clausen, H.B., Dahl-Jensen, D., Fischer, H., Goto-Azuma, K., Hansson, M., Johnsen, S.J., Jouzel, J., Masson-Delmotte, V., Popp, T., Rasmussen, S.O., Röthlisberger, R., Ruth, U., Stauffer, B., Siggaard-Andersen, M.L., Sveinbjörnsdóttir, A.E., Svensson, A., White, J.W.C., 2008. High-resolution Greenland ice core data show abrupt climate change happens in few years. *Science* 321, 680-684.

Stocker, T.F., Johnsen, S.J., 2003. A minimum thermodynamic model for the bipolar seesaw. *Paleoceanography* 18, doi: 10.1029/2003PA000920.

Stokes, M.A., Smiley, T.L., 1968. *An Introduction to Tree-Ring Dating*. University of Chicago Press Chicago.

Svensson, G., 1988. Bog development and environmental conditions as shown by the stratigraphy of Store Mosse mire in southern Sweden. *Boreas* 17, 89-111.

Tarasov, L., Peltier, W.R., 2005. Arctic freshwater forcing of the Younger Dryas cold reversal. *Nature* 435, 662-665.

- Theiler, J., Eubank, S., Longtin, A., Galdrikian, B., Doyne Farmer, J., 1992. Testing for nonlinearity in time series: the method of surrogate data. *Physica D: Nonlinear Phenomena* 58, 77-94.
- Thomas, Z.A., Kwasniok, F., Boulton, C.A., Cox, P.M., Jones, R.T., Lenton, T.M., Turney, C.S.M., 2015. Early warnings and missed alarms for abrupt monsoon transitions. *Clim. Past* 11, 1621-1633.
- Tierney, J.E., Abram, N.J., Anchukaitis, K.J., Evans, M.N., Giry, C., Kilbourne, K.H., Saenger, C.P., Wu, H.C., Zinke, J., 2015. Tropical sea surface temperatures for the past four centuries reconstructed from coral archives. *Paleoceanography* 30, 226-252.
- Trenberth, K.E., Shea, D.J., 1987. On the evolution of the Southern Oscillation. *Monthly Weather Review* 115, 3078-3096.
- Trouet, V., Scourse, J.D., Raible, C.C., 2012. North Atlantic storminess and Atlantic Meridional Overturning Circulation during the last Millennium: Reconciling contradictory proxy records of NAO variability. *Global and Planetary Change* 84–85, 48-55.
- Tudhope, A.W., Chilcott, C.P., McCulloch, M.T., Cook, E.R., Chappell, J., Ellam, R.M., Lea, D.W., Lough, J.M., Shimmield, G.B., 2001. Variability in the El Niño-Southern Oscillation through a glacial-interglacial cycle. *Science* 291, 1511-1517.
- Turney, C.S.M., Fifield, L.K., Hogg, A.G., Palmer, J.G., K., H., Baillie, M.G.L., Galbraith, R., Ogden, J., Lorrey, A., Tims, S., Jones, R.T., 2010. Using New Zealand kauri (*Agathis australis*) to test the synchronicity of abrupt climate change during the Last Glacial Interval (60,000-11,700 years ago). *Quaternary Science Reviews* 29, 3677-3682.
- Turney, C.S.M., Fogwill, C.J., Klekociuk, A.R., van Ommen, T.D., Curran, M.A.J., Moy, A.D., Palmer, J.G., 2015. Tropical and mid-latitude forcing of continental Antarctic temperatures. *The Cryosphere* 9, 2405-2415.
- Turney, C.S.M., Hobbs, D., 2006. ENSO influence on Holocene Aboriginal populations in Queensland, Australia. *Journal of Archaeological Science* 33, 1744-1748.
- Turney, C.S.M., Jones, R.T., Lister, D., Jones, P., Williams, A.N., Hogg, A., Thomas, Z.A., Compo, G.P., Yin, X., Fogwill, C.J., Palmer, J., Colwell, S., Allan, R., Visbeck, M., 2016a. Anomalous mid-twentieth century atmospheric circulation change over the South Atlantic compared to the last 6000 years. *Environmental Research Letters* 11, 64009-64022.
- Turney, C.S.M., Kershaw, A.P., Lowe, J.J., van der Kaars, S., Johnston, R., Rule, S., Moss, P., Radke, L., Tibby, J., McGlone, M.S., Wilmshurst, J.M., Vandergoes, M.J., Fitzsimons, S.J., Bryant, C., James, S., Branch, N.P., Cowley, J., Kalin, R.M., Ogle, N., Jacobsen, G.,

- 1 Fifeild, L.K., 2006. Climatic variability in the southwest Pacific during the Last
- 2 Termination (20-10 ka BP). *Quaternary Science Reviews* 25, 886-903.
- 3 Turney, C.S.M., McGlone, M.S., Wilmshurst, J.W., 2003. Asynchronous climate change
- 4 between New Zealand and the northern Atlantic during the last deglaciation. *Geology* 31,
- 5 223-226.
- 6 Turney, C.S.M., Palmer, J., 2007. Does the El Niño-Southern Oscillation control the
- 7 interhemispheric radiocarbon offset? *Quaternary Research* 67, 174-180.
- 8 Turney, C.S.M., Palmer, J., Bronk Ramsey, C., Adolphi, F., Muscheler, R., Hughen, K.A.,
- 9 Staff, R.A., Jones, R.T., Thomas, Z.A., Fogwill, C.J., Hogg, A., 2016b. High-precision
- 10 dating and correlation of ice, marine and terrestrial sequences spanning Heinrich Event 3:
- 11 Testing mechanisms of interhemispheric change using New Zealand ancient kauri
- 12 (*Agathis australis*). *Quaternary Science Reviews* 137, 126-134.
- 13 Ummenhofer, C.C., England, M.H., 2007. Interannual extremes in New Zealand precipitation
- 14 linked to modes of Southern Hemisphere climate variability. *Journal of Climate* 20, 5418-
- 15 5440.
- 16 van Nes, Egbert H., Scheffer, M., 2007. Slow recovery from perturbations as a generic
- 17 indicator of a nearby catastrophic shift. *The American Naturalist* 169, 738-747.
- 18 van Oldenborgh, G.J., Burgers, G., 2005. Searching for decadal variations in ENSO
- 19 precipitation teleconnections. *Geophysical Research Letters* 32, L15701, doi:
- 20 15710.11029/12005GL023110.
- 21 Vandergoes, M.J., Dieffenbacher-Krall, A.C., Newnham, R.M., Denton, G.H., Blaauw, M.,
- 22 2008. Cooling and changing seasonality in the southern Alps, New Zealand during the
- 23 Antarctic cold reversal. *Quaternary Science Reviews* 27, 589-601.
- 24 Vogel, J.S., Southon, J.R., Nelson, D., Brown, T.A., 1984. Performance of catalytically
- 25 condensed carbon for use in accelerator mass spectrometry. *Nuclear Instruments and*
- 26 *Methods in Physics Research Section B: Beam Interactions with Materials and Atoms* 5,
- 27 289-293.
- 28 WAIS Divide Project Members, 2015. Precise inter polar phasing of abrupt climate change
- 29 during the last ice age. *Nature* 520, 661-665.
- 30 Walker, M.J.C., Björck, S., Lowe, J.J., Cwynar, L.C., Johnsen, S., Knudsen, K.-L., Wohlfarth,
- 31 B., INTIMATE group, 1999. Isotopic 'events' in the GRIP ice core: a stratotype for the late
- 32 Pleistocene. *Quaternary Science Reviews* 18, 1143-1150.

- 1 Walker, M.J.C., Coope, G.R., Sheldrick, C., Turney, C.S.M., Lowe, J.J., Blockley, S.P.E.,
2 Harkness, D.D., 2003. Devensian Lateglacial environmental changes in Britain: A multi-
3 proxy record from Llanilid, south Wales, UK. *Quaternary Science Reviews* 22, 475-520.
- 4 Wang, Y.J., Cheng, H., Edwards, R.L., An, Z.S., Wu, J.Y., Shen, C.C., Dorale, J.A., 2001. A
5 high-resolution absolute-dated Late Pleistocene monsoon record from Hulu Cave, China.
6 *Science* 294, 2345-2348.
- 7 Wigley, T.M.L., Briffa, K.R., Jones, P.D., 1984. On the average value of correlated time
8 series with applications in dendroclimatology and hydrometeorology. *Journal of Climate*
9 *and Applied Meteorology* 23, 201-213.
- 10 Williams, J.W., Post, D.M., Cwynar, L.C., Lotter, A.F., Levesque, A.J., 2002. Rapid and
11 widespread vegetation responses to past climate change in the North Atlantic region.
12 *Geology* 30, 971-974.
- 13 Xie, R., Huang, F., Jin, F.-F., Huang, J., 2015. The impact of basic state on quasi-biennial
14 periodicity of central Pacific ENSO over the past decade. *Theor Appl Climatol* 120, 55-67.
- 15 Yoshida, A., Takeuti, S., 2009. Quantitative reconstruction of palaeoclimate from pollen
16 profiles in northeastern Japan and the timing of a cold reversal event during the Last
17 Termination. *Journal of Quaternary Science* 24, 1006-1015.

Figure 1

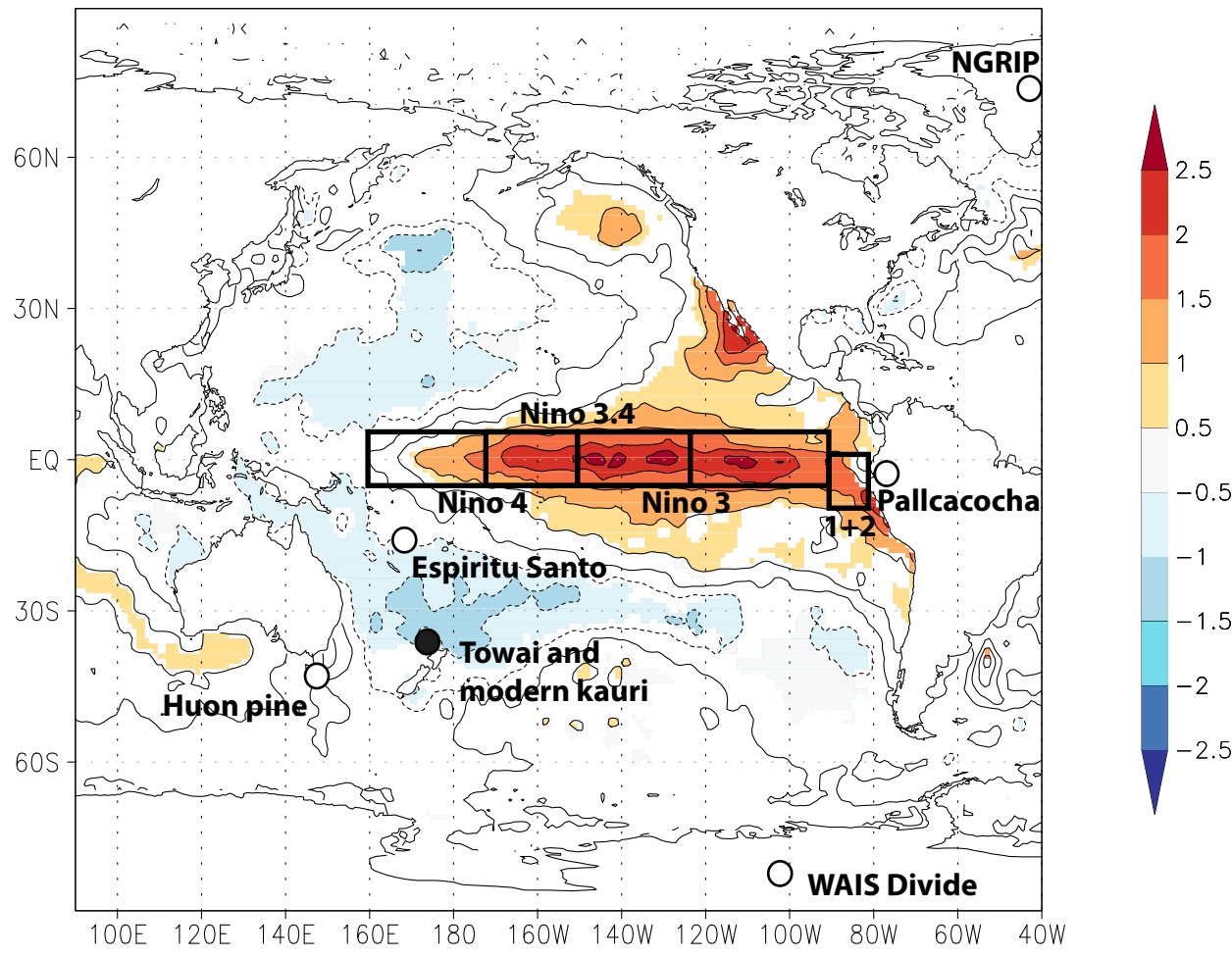


Figure 2

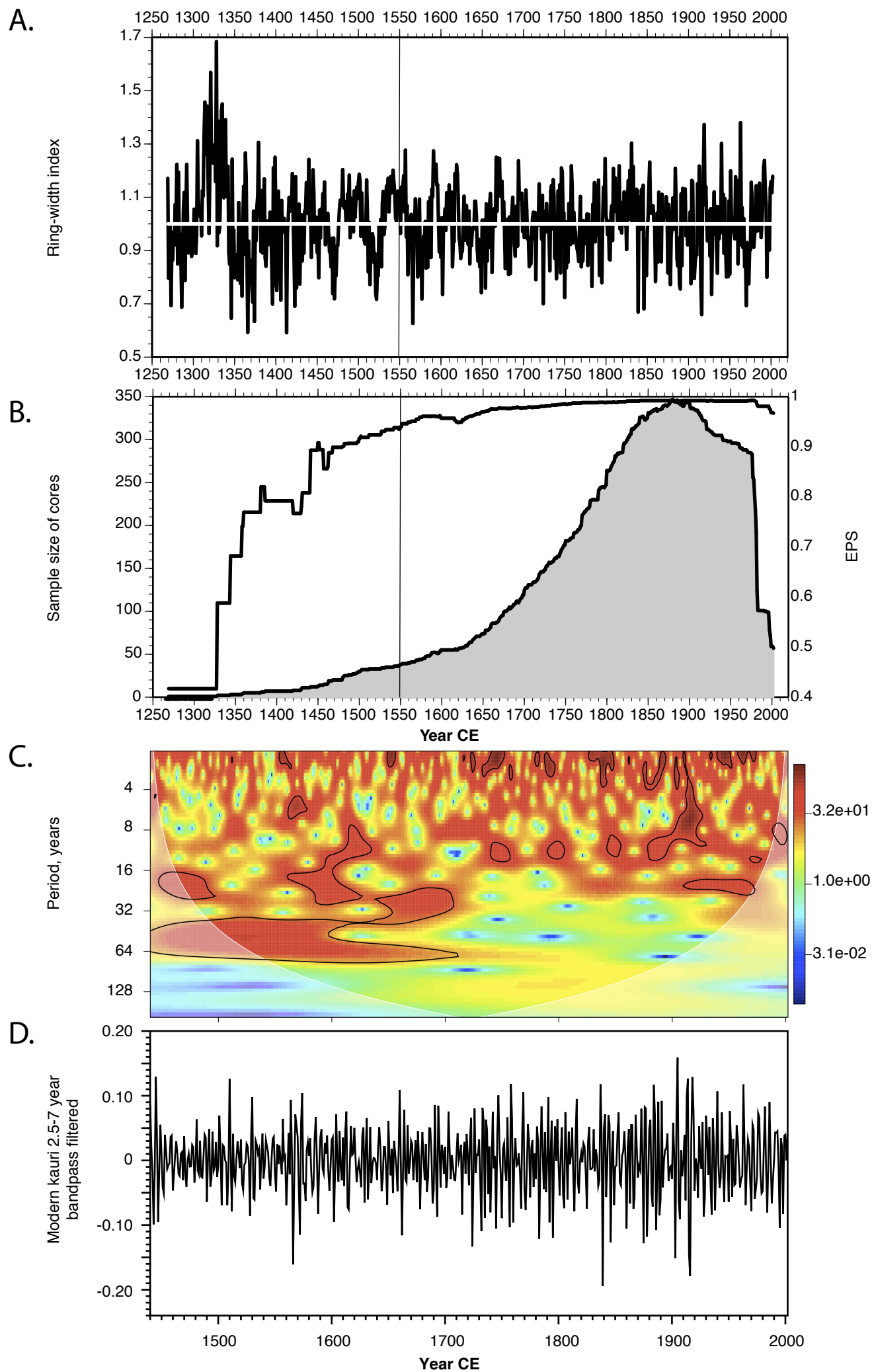


Figure 3

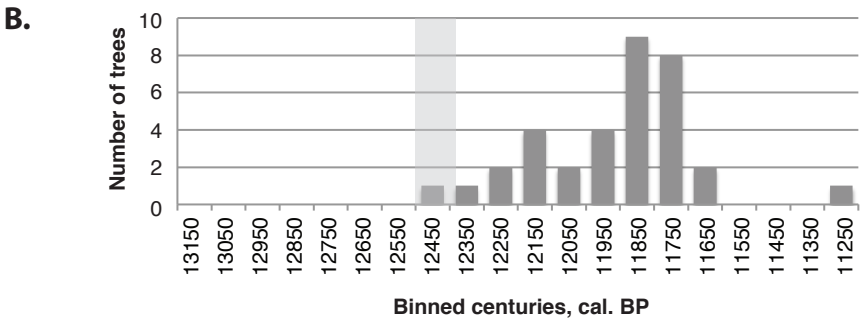
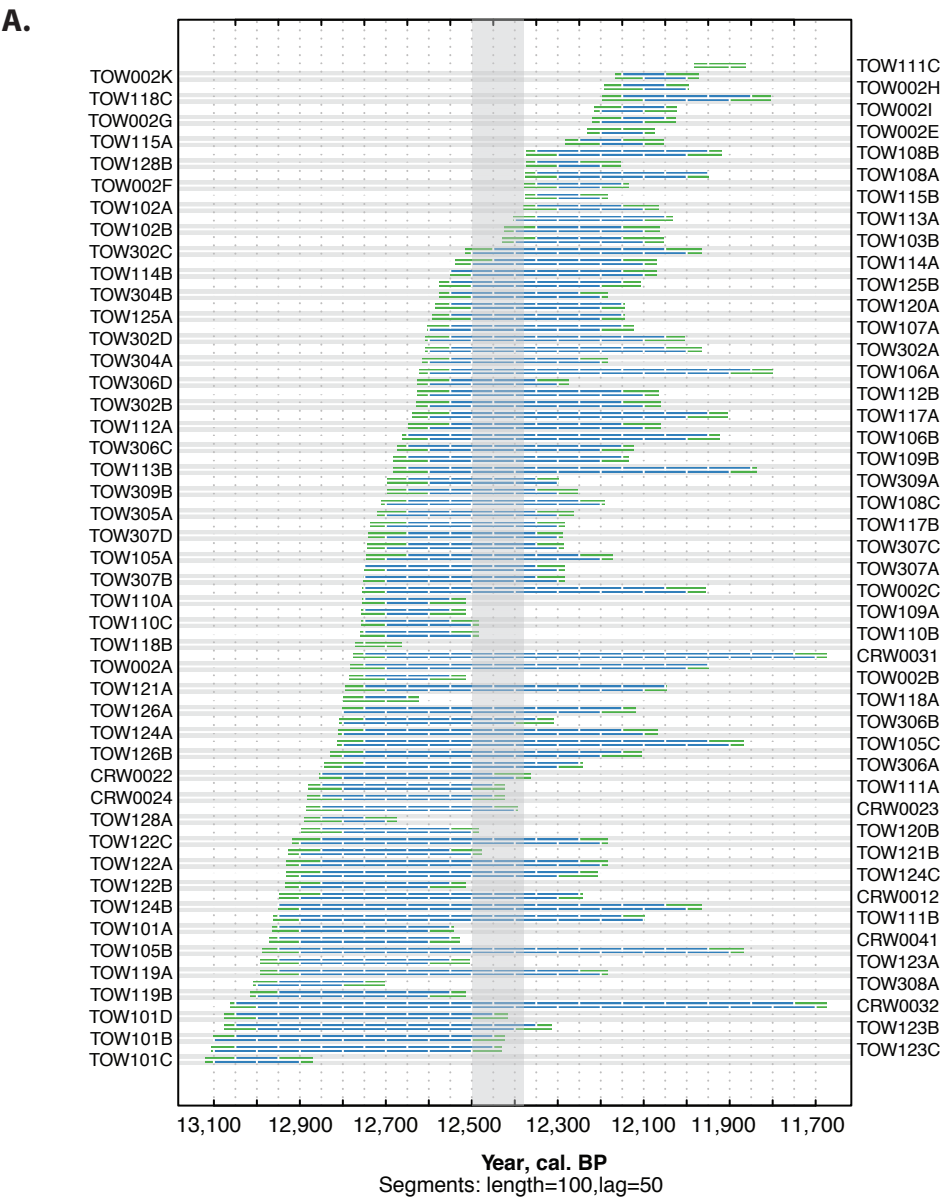
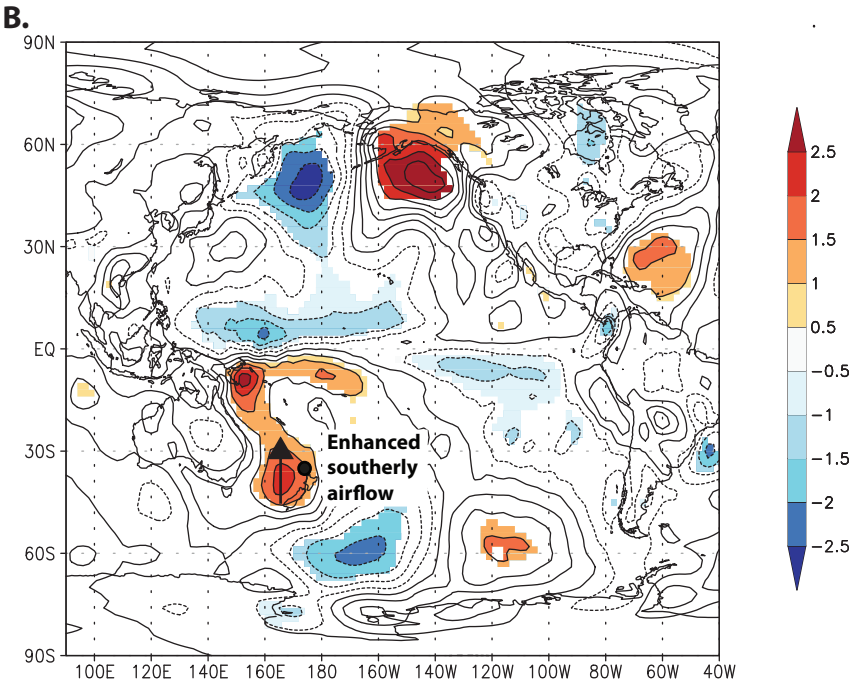
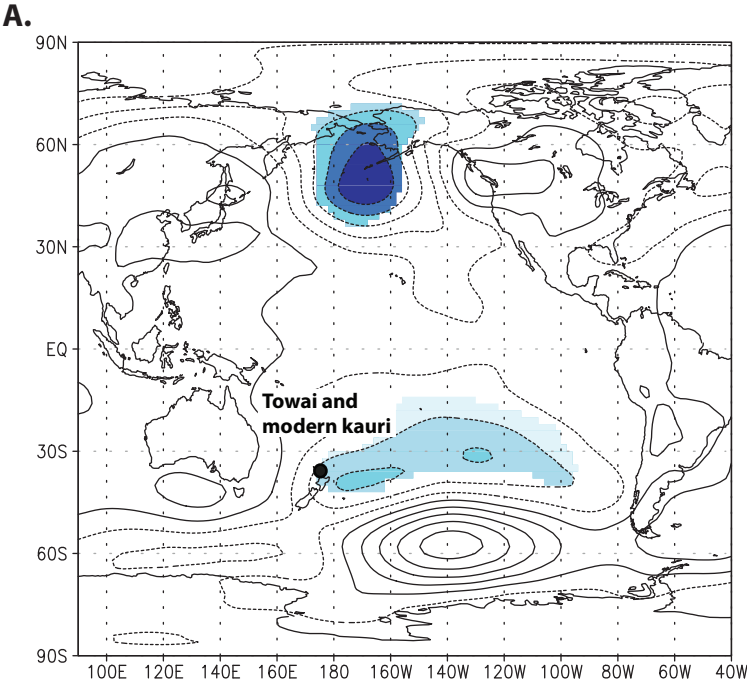


Figure 4

ZERO LAG



KAURI
2 MONTH
LAG

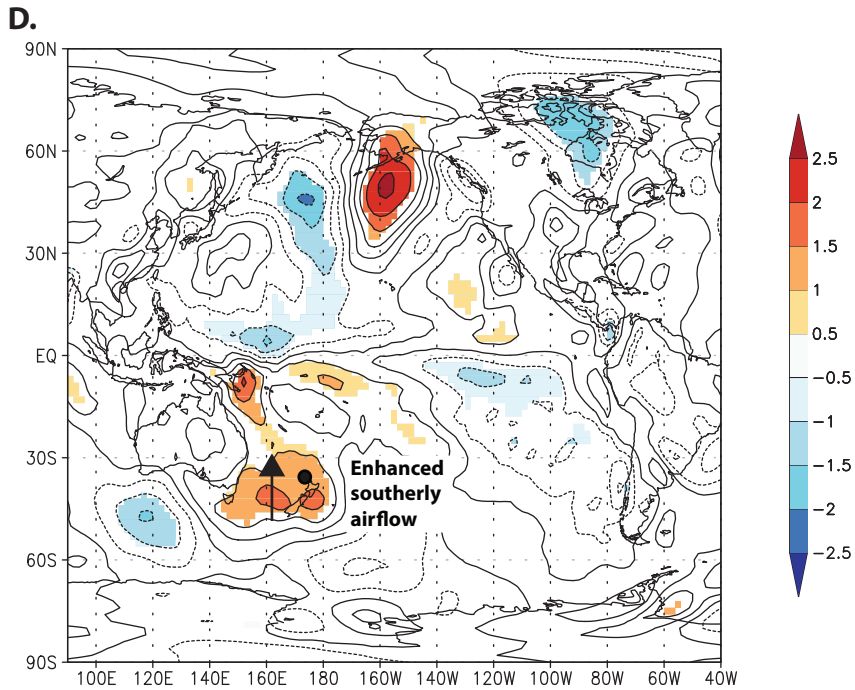
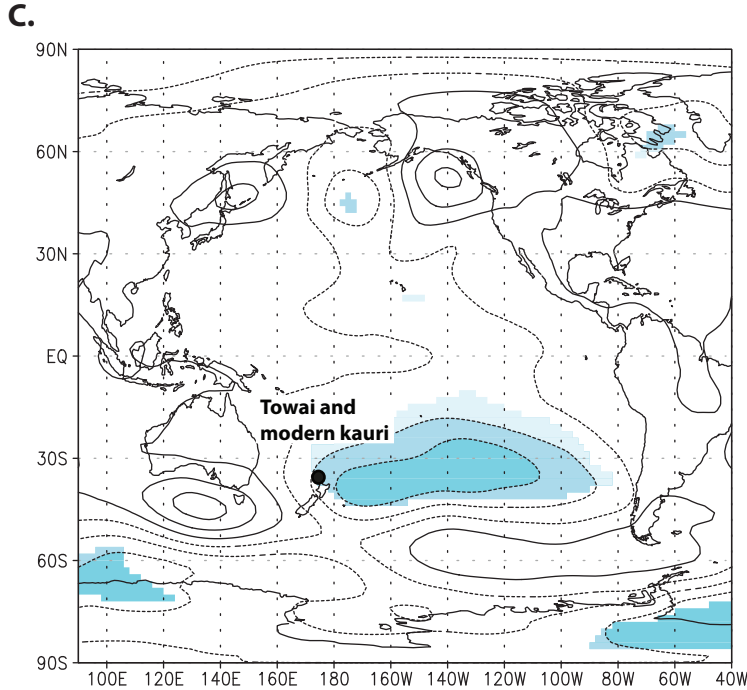


Figure 5

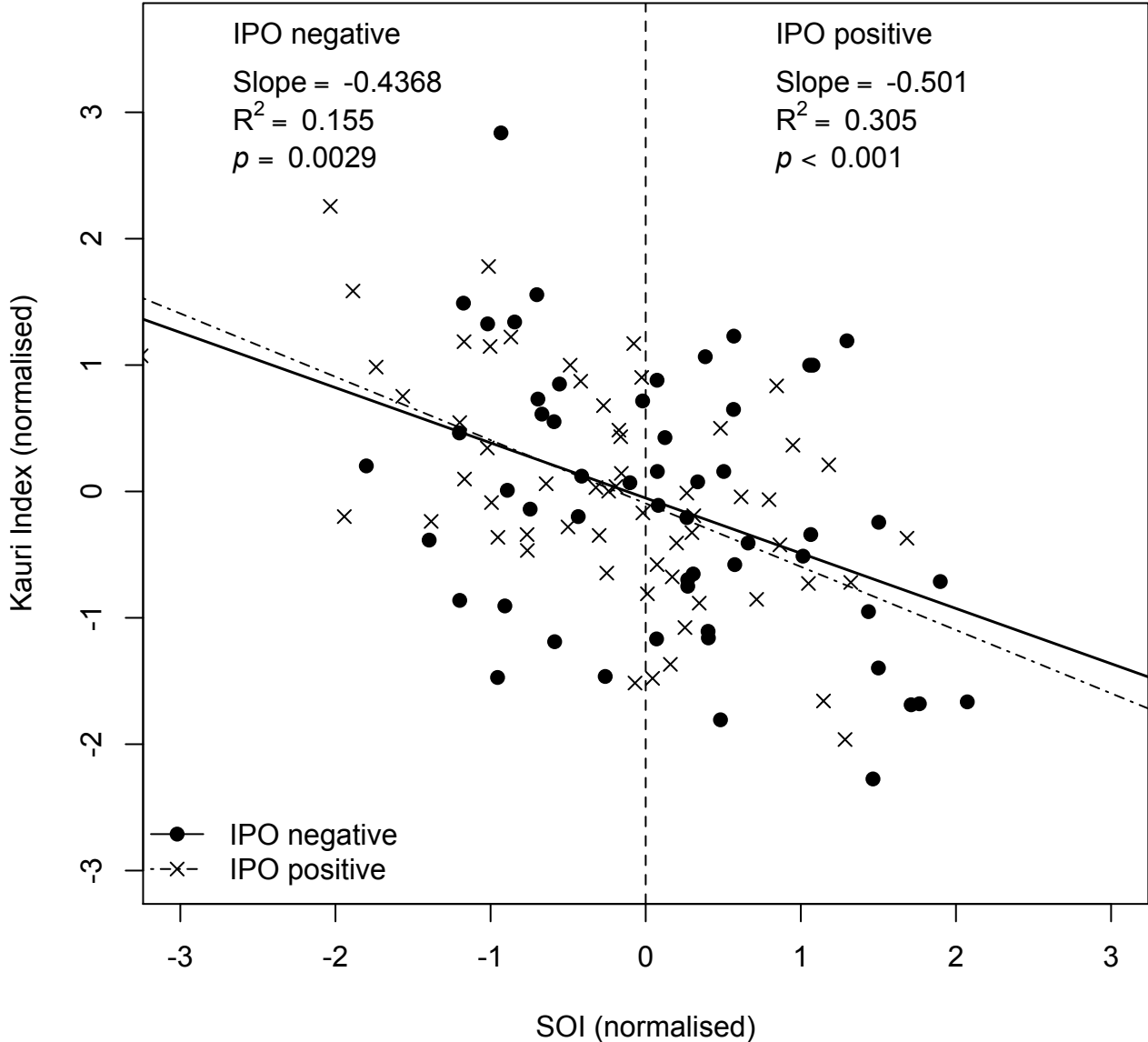


Figure 6

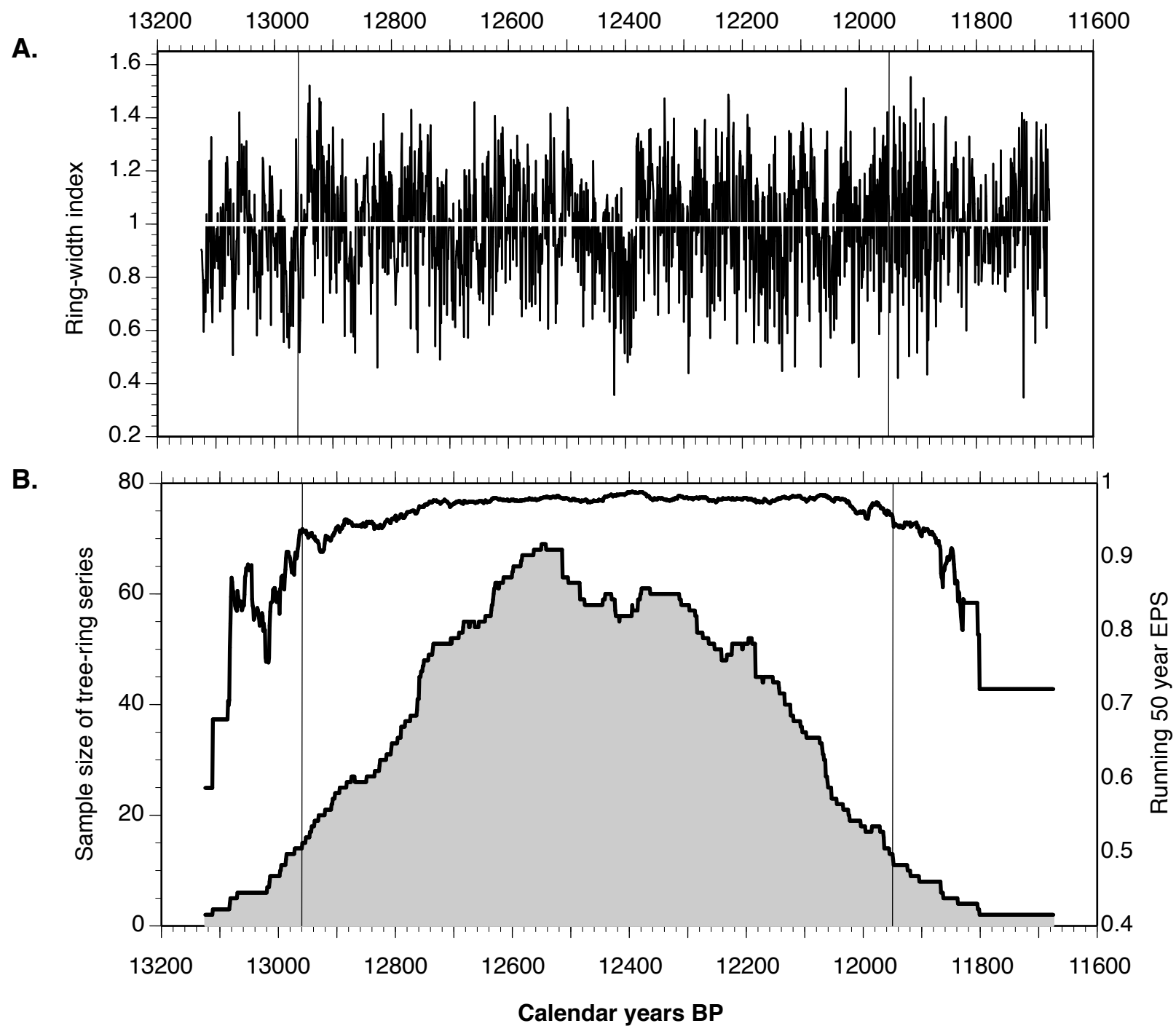


Figure 7

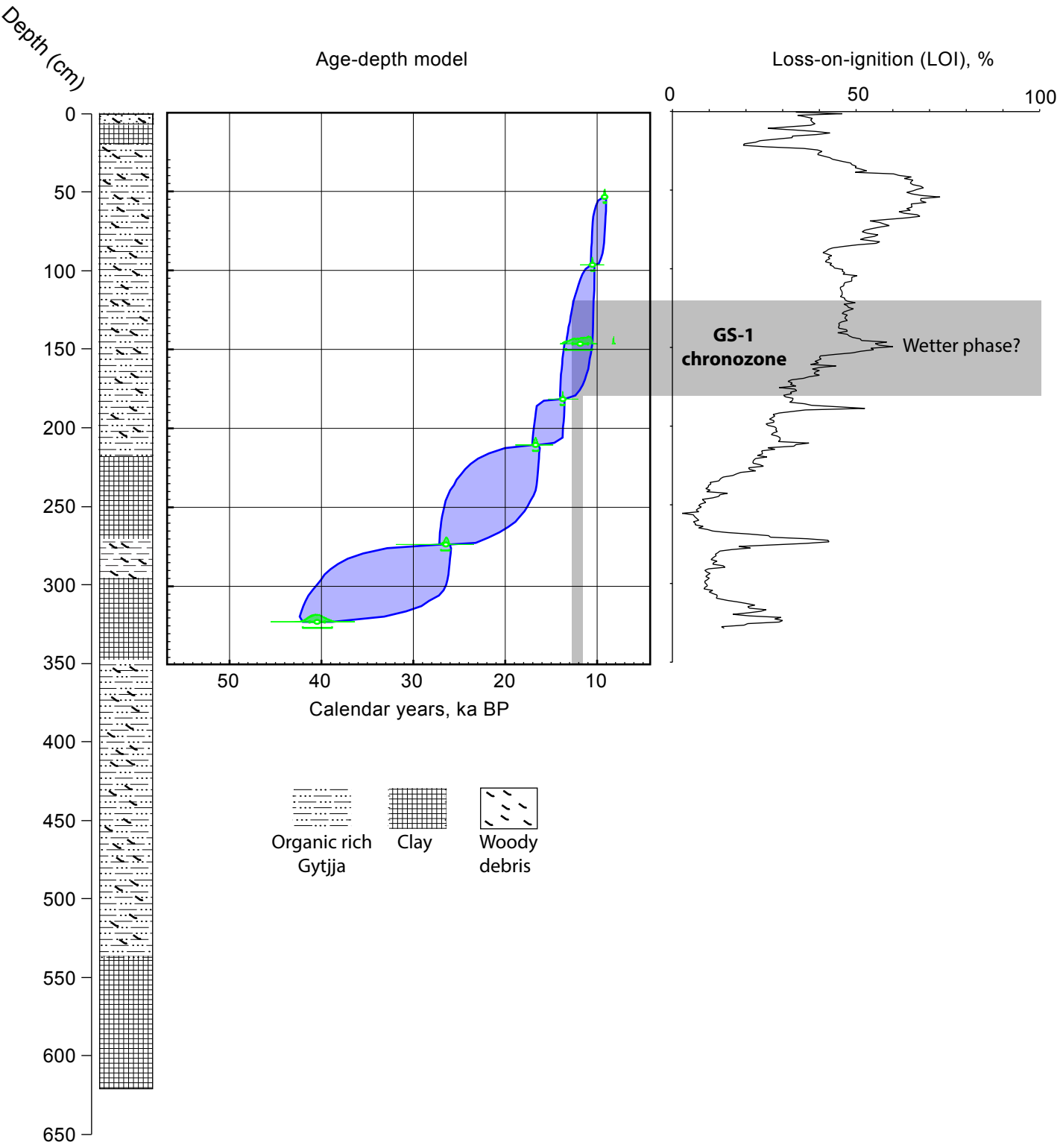


Figure 8

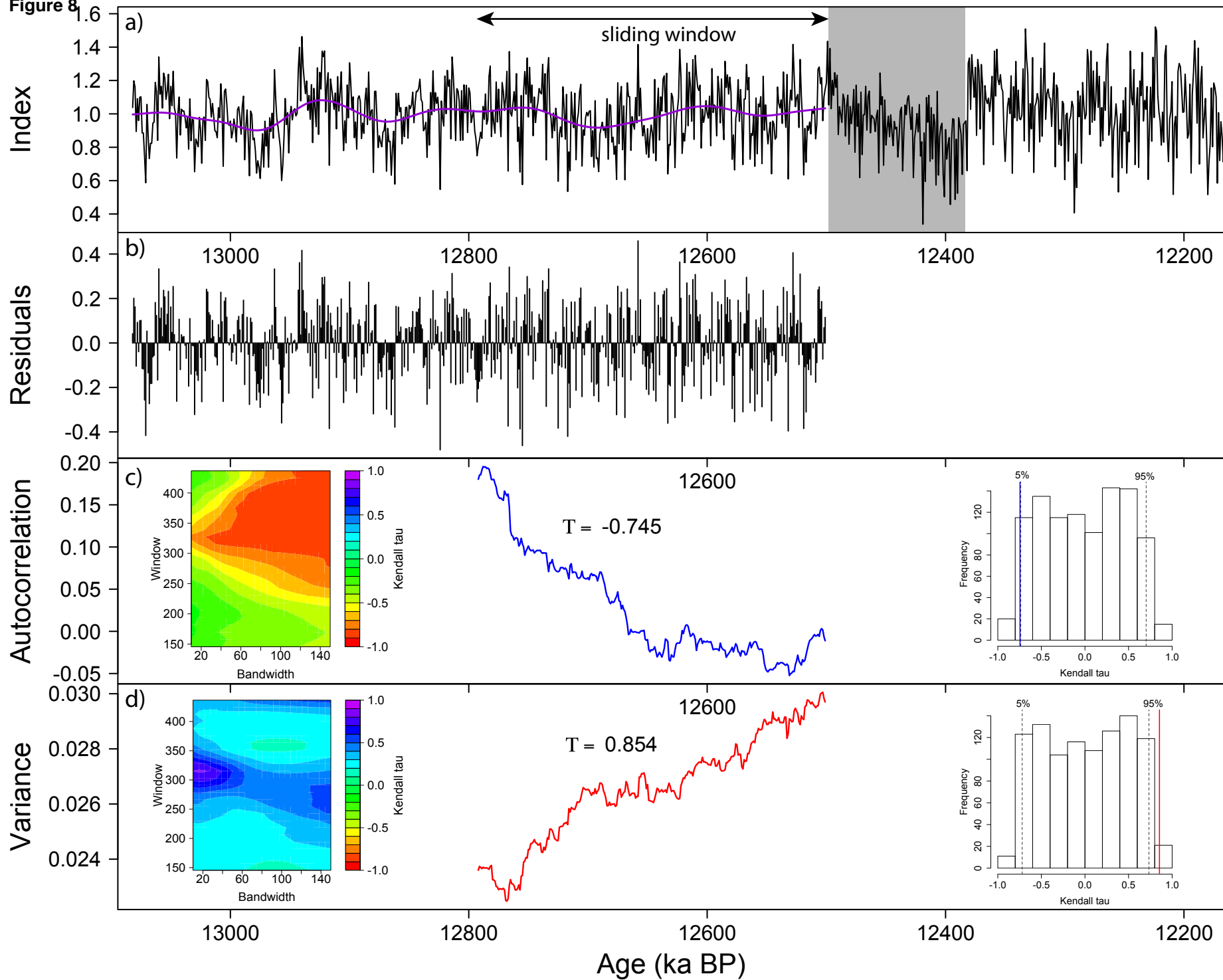


Figure 9

